Physics – Uspekhi **55** (11) 1080 – 1097 (2012)

REVIEWS OF TOPICAL PROBLEMS PACS numbers: 41.20.Jb, 42.70.Qs, **73.20. – r**

Light propagation in composite materials with gain layers

A V Dorofeenko, A A Zyablovsky, A A Pukhov, A A Lisyansky A P Vinogradov

DOI: 10.3367/UFNe.0182.201211b.1157

Contents

1. Introduction **1080**
2. Description of a gain medium using the dielectric constant with a negative imaginary part **1081**
3. Normal incidence of light on a gain medium **1082**
3.1 History of the problem; 3.2 Fresnel and Airy approaches; 3.3 Temporal problem of the propagation of a semi-infinite wave train through a gain layer
4. Lasing in photonic crystals **1089**
4.1 Airy series for photonic crystals; 4.2 Lasing in the allowed band of photonic crystals; 4.3 Lasing in the forbidden band of a photonic crystal
5. Oblique incidence of light on a gain layer **1093**
6. Conclusions **1094**
References **1096**

Abstract. Light propagation through a single gain layer and a multilayer system with gain layers is studied. Results obtained using the Fresnel formulas, Airy's series summation, and the numerical solution of the nonlinear Maxwell–Bloch equations by the finite difference time domain (FDTD) method are analyzed and compared. Normal and oblique propagation of a wave through a gain layer and a slab of a photonic crystal are examined. For the latter problem, the gain line may be situated in either the pass or stop band of the photonic crystal. It is shown that the monochromatic plane-wave approximation is generally inapplicable for active media, because it leads to results that violate causality. But the problem becomes physically meaningful and correct results can be obtained for all three approaches once the structure of the wavefront and the finite aperture of the beam are taken into account.

1. Introduction

The problem of light propagation through a system of gain layers is of great applied and fundamental importance. Applied problems are related to the development of semiconductor vertical cavity surface-emitting lasers (VCSELs) [1–6]. Multilayer gain systems are often used as model media for studying Anderson localization of light [7–17] and lasing in random media [18–20]. Fundamental investigations of metamaterials [21–23] have rekindled recent interest in problems of light propagation through multilayer gain systems. In addition, this problem is of great methodological importance because the neglect of diffraction phenomena and the one-dimensionality of the problem allow obtaining analytic solutions.

The choice of the scope of phenomena considered in this review assumes the use of the results obtained here for analyzing the properties of metamaterials containing layers with gain elements [23–27].

The unique properties of metamaterials (negative values of the magnetic permeability and the dielectric constant) appear due to a plasmon resonance in metal nanoparticles embedded into materials. The signs of the impedance and refractive index are not important in the phenomena considered here, and therefore we do not focus on media with negative absorption, referring to recent reviews [28, 29], where different approaches to the solution of this problem are discussed.

Almost all potential applications require metamaterials with very low losses [30], which cannot be achieved in passive systems at present. To reduce losses, it was proposed to combine metamaterials with gain media (see [23, 25, 26, 31–34] and review [35] and the references therein). In particular, the authors of [23] proposed alternating metamaterial layers with gain-medium layers (the Pendry–Ramakrishna scheme). In [33, 36], it was proposed to embed gain elements directly into a metamaterial matrix.

The aim of this review is to describe the physical picture of the propagation of an electromagnetic wave through multilayer systems containing gain layers. Special attention is devoted to the linear stage of interaction with the field of the incident wave, i.e., before the onset of lasing. For this, we describe gain media using the dielectric constant with a negative imaginary part. The interaction of the system with the wave is calculated by two methods: based on boundary

A V Dorofeenko, A A Zyablovsky, A A Pukhov, A P Vinogradov
Institute for Theoretical and Applied Electrodynamics,
Russian Academy of Sciences,
ul. Izhorskaya 13, 125412 Moscow, Russian Federation,
Moscow Institute of Physics and Technology (State University),
Institutskii per. 9, 141700 Dolgoprudnyi, Moscow region,
Russian Federation. Tel. +7 (968) 636 96 13, +7 (495) 485 83 55
E-mail: alexandor7@gmail.com, zyablovskiy@mail.ru,
pukhov@mail.ru, a-vinogr@yandex.ru
A A Lisyansky Physics Department, Queens College of the City University of New York, Flushing, 11367, New York, USA
Tel. (718) 997 33 71. E-mail: alexander.lisyansky@qc.cuny.edu

Received 27 October 2010, revised 16 July 2012
Uspekhi Fizicheskikh Nauk **182** (11) 1157 – 1175 (2012)
DOI: 10.3367/UFNr.0182.201211b.1157
Translated by M Sapozhnikov; edited by A M Semikhatov

conditions for the total field (Fresnel's method) and by analyzing the propagation of the wave as the rereflection process (Airy's method). The results are controlled by comparing them with the numerical solution of 'straightforward' nonlinear Maxwell–Bloch equations describing the interaction of a classical electromagnetic field with a quantum-mechanical system (atom, molecule, or quantum dot) with inverted population [37]. In what follows, for clarity, we take the quantum mechanical system to be a quantum dot (QD). As is shown here (see also [24, 38, 39]), in the absence of lasing in the limit of weak fields, the propagation of a wave can be described by the Maxwell equations by introducing a negative imaginary part $\mathrm{Im}\,\varepsilon < 0$ of the dielectric constant. The simplicity of such an approach makes it attractive for theoretical studies of gain media [40–44]. In addition, this approach is most often used for analyzing experiments with metamaterials [25, 26, 45].

The possibility of describing the propagation of an electromagnetic wave through a sample in terms of a linear dielectric constant $\varepsilon_{\mathrm{gain}}(\omega)$, which we consider in this review, is very important both for applications (considerably simplifying the design of particular devices) and for processing experimental results (the electromagnetic properties of metamaterials are described in modern models by introducing the effective dielectric constant of metamaterials). Indeed, most investigations of the properties of metamaterials with gain components assume that these metamaterials are linear media [27, 46–48]. In other words, the authors of these papers considered either subthreshold or intermediate states before the onset of stationary lasing in metamaterials. Such an approach is exhausted by these two cases, because lasing transforms a metamaterial with gain into a nonlinear object.

Typically, the coefficients of transmission T and reflection R of light from a layer are measured in experiments. The algorithm for determining the refractive index and impedance or, alternatively, the dielectric constant and magnetic permeability of a material from data for R and T is based on Fresnel formulas: more precisely, on the solution of a one-dimensional wave equation [49–55]. In the case of 'right-hand' media, no problems appear. In the case of 'left-hand' media, where the dielectric constant and magnetic permeability are negative [22], the procedure for obtaining homogenized values of the effective dielectric constant $\varepsilon_{\mathrm{eff}}(\varepsilon)$ and $\mu_{\mathrm{eff}}(\varepsilon)$ from $R(\varepsilon)$ and $T(\varepsilon)$ is ambiguous. This is because of the ambiguity of the separation of the analytic branch of the square root of a function of two complex variables [28]. In contrast to the case of one complex variable [56], the complex analysis does not give an unambiguous recipe for separating the analytic branch of a function of two complex variables. A physically consistent approach was developed for passive media: the square root of a product of complex factors $\sqrt{Z_1 Z_2}$ is defined as the product of square roots of each factor, $\sqrt{Z_1}\sqrt{Z_2}$ [57]. The 'correct' branch of the square root is chosen based on physical considerations: the real part $\mathrm{Re}\,Z$ of the input impedance should be positive [58]. In the case of gain media, the question of the sign of the real part of the input impedance remains open [28] because the amplitude of the reflected wave can exceed that of the incident wave. Indeed, the authors of [59, 60] studied the oblique incidence of light on a gain medium under the conditions of total internal reflection and observed a reflection coefficient higher than unity. This fact in itself is not unexpected because in the case of total internal reflection, a wave, before reflecting, partially enters into the gain medium [61, 62]. But the question of whether an energy flux can emerge from a sample toward the incident wave ($\mathrm{Re}\,Z < 0$) in the case of small angles of incidence (in particular, in the case of normal incidence) requires a separate consideration.

The description of a gain medium using the dielectric constant is well justified for the Pendry–Ramakrishna scheme, where regions with a gain material and regions containing plasmon nanoparticles are separated. But when inverted QDs are embedded directly into a matrix surrounding metal nanoparticles, a quantum problem of the excitation of an inverted QD of a surface plasmon localized on a nanoparticle arises. In fact, a nanoparticle + QD pair forms a spaser (an acronym for surface plasmon amplification by stimulated emission of radiation) [63], which has been extensively studied recently. The solution to the problem of the interaction of a system of spasers above the lasing threshold with an electromagnetic wave propagating in a metamaterial requires other approaches taking both quantum and nonlinear properties of the spaser into account. These questions are not considered here, and have been analyzed in [64–70].

We note that the interpretation of experimental data obtained at present [25, 71] is complicated by the fact that samples used in [25, 71] had features of both schemes: as a rule, inverted QDs are deposited on a prepared sample of a metamaterial [71].

Interest in states preceding the onset of lasing is explained by the fact that losses and gains are equally destructive for applications of metamaterials. Indeed, devices based on metamaterials, in particular, a superlens [21], which uses metamaterials to go beyond the diffraction limit, are typically near-field devices. Energy transfer by near fields (inhomogeneous waves or evanescent modes) has a certain specificity [72, 73]: one inhomogeneous wave does not transfer energy because the electric and magnetic fields in it are shifted by a quarter of a period [74], and the Poynting vector identically vanishes. To transfer energy, a second (reflected) near-field wave is required. The contribution to the energy transfer is given by cross (interference) terms appearing due to the overlap of the magnetic field of one wave and the electric field of another; we note that the nonzero energy flux can form only if these waves have a phase difference [72]. The converse is also true: the appearance of an energy flux leads to a phase shift between 'interfering' near fields. The presence of losses or gains produces the energy flux in this system. As a result, a phase shift appears in a layer of a metamaterial, which is not envisaged in the 'scheme without losses' and typically depends on the wave number of the evanescent harmonic. The destructive interference appearing in this case results in a partial or complete destruction of a super image [75]. Hence, an exact compensation of losses is needed, and subthreshold states are of most interest here. In this case, there is hope to create metamaterials in which losses in a metal are compensated due to the energy flux from QDs before the development of lasing.

2. Description of a gain medium using the dielectric constant with a negative imaginary part

Before proceeding to the study of peculiarities of light propagation in a gain medium, we consider the possibility of

reducing the originally quantum problem to a semiclassical problem, i.e., to the use of the dielectric constant with a negative imaginary part $\operatorname{Im}\varepsilon_{\text{gain}}(\omega) < 0$. The presence of a large number of photons in the radiation modes considered here allows neglecting quantum fluctuations and describing the electromagnetic field by the classical Maxwell equations [76, 77]. At the same time, the behavior of the two-level system modeling a QD requires quantum mechanical treatment. This approximation is called semiclassical, and the corresponding system of equations is called the Maxwell–Bloch equations. In the one-dimensional case, where all physical quantities depend only on the coordinate z and time, and a wave propagates normally the metamaterial layers, these equations take the form [37, 39, 78–80]

$$\begin{aligned}
&\frac{\partial^2 E}{\partial z^2} - \frac{\varepsilon_0(z)}{c^2}\frac{\partial^2 E}{\partial t^2} = \frac{4\pi}{c^2}\frac{\partial^2 P}{\partial t^2}\,,\\
&\frac{\partial^2 P}{\partial t^2} + \frac{2}{\tau_{\text{P}}}\frac{\partial P}{\partial t} + \omega_0^2 P = -\frac{2\omega_0|\mu|^2 nE}{\hbar}\,,\\
&\frac{\partial n}{\partial t} + \frac{1}{\tau_n}(n - n_0) = \frac{2}{\hbar\omega_0}\,E\frac{\partial P}{\partial t}\,.
\end{aligned} \tag{1}$$

Here, the electric field $E(z,t)$, the polarization $P(z,t)$, the dielectric constant $\varepsilon_0(z)$ of a matrix, and the population inversion n for the upper and lower level of a QD are assumed to be real quantities. The external excitation tends to bring n to n_0, while stimulated emission reduces n. Next, ω_0 is the transition frequency of a QD, μ is an off-diagonal element of the transition dipole moment of the QD, and τ_{P} and τ_n are the respective characteristic relaxation times for polarization and population inversion. The population inversion relaxation (transverse relaxation) is related to the same processes and elastic processes, which do not change the population inversion, but change the polarization phase. Therefore, the transverse relaxation time is always shorter than the longitudinal relaxation time [79].

The first equation of system (1) is a wave equation obtained from the Maxwell equations for an inhomogeneous medium. The other two equations are obtained from equations for the density matrix of the QD and describe the polarization and inverse population of QDs [78, 81, 82].

Passing to the Fourier representation, we write the right-hand side of the last equation in (1) in the form (see [58])

$$\frac{1}{2\hbar\omega_0}\left(E^*\frac{\partial P}{\partial t} + E\frac{\partial P^*}{\partial t}\right).$$

In this case, $n(z)$ is no longer dependent on time. The variables P and n can be eliminated to obtain a single equation for the electric field:

$$\frac{\partial^2 E(z,\omega)}{\partial z^2} + \left(\frac{\omega}{c}\right)^2 \varepsilon_{\text{gain}}(\omega)\,E(z,\omega) = 0\,. \tag{2a}$$

The gain medium is then described by the effective dielectric constant

$$\varepsilon_{\text{gain}}(\omega) = \varepsilon_0 + \alpha\,\frac{\omega_0}{\omega}\,\frac{-\mathrm{i} + (\omega^2 - \omega_0^2)/(2\omega/\tau_{\text{P}})}{1 + \beta|E|^2 + \left[(\omega^2 - \omega_0^2)/(2\omega/\tau_{\text{P}})\right]^2} \tag{2b}$$

with a negative imaginary part for $n_0 > 0$ (see also [39, 83–85]). Here, $\alpha = 4\pi|\mu|^2\tau_{\text{P}}n_0/\hbar$ and $\beta = |\mu|^2\tau_n\tau_{\text{P}}/\hbar^2$.

Because of the dependence of $\varepsilon_{\text{gain}}$ on E, Eqn (2a) is a nonlinear Helmholtz equation describing the distribution of the harmonic field $E(z,\omega)$ over z. The decrease in the imaginary part of $\varepsilon_{\text{gain}}(\omega)$ with increasing the field strength $E(z,\omega)$ is caused by the suppression of the population inversion in QDs due to stimulated emission. However, if the field strength is small,

$$|E|^2 \ll \frac{\hbar^2}{|\mu|^2\tau_{\text{P}}\tau_n}\,, \tag{2c}$$

then the propagation of the wave in the gain medium can be described using a field-independent dielectric constant with the frequency dispersion having an 'anti-resonance' form and a negative imaginary part:

$$\varepsilon_{\text{gain}}(\omega) = \varepsilon_0 - \frac{2\alpha\omega_0/\tau_{\text{P}}}{-2\mathrm{i}\omega/\tau_{\text{P}} + \omega_0^2 - \omega^2}\,. \tag{2d}$$

We note that the use of nonlinear Helmholtz equation (2a) allows taking the influence of the field intensity on the properties of the medium into account only below the lasing threshold. This is explained by the fact that lasing typically begins to develop at a frequency different from the incident wave frequency (see, e.g., [86]).

3. Normal incidence of light on a gain medium

3.1 History of the problem

The problem of the reflection of a plane wave normally incident on a gain medium has a long history [40–44], which is full of contradictions and unclear points. In particular, the author of [42] theoretically studied the reflection of a wave from the interface of two media, one of which was a gain medium. First, the propagation of the wave through a finite-thickness gain layer was considered, and the reflection coefficient was found by solving the one-dimensional wave equation with Maxwell's boundary conditions [87]. Below, we call such an approach the Fresnel approach. Then a passage to the limit of a semi-infinite layer was performed [42]. The reflection coefficient R of the gain half-space found in this way turns out to be greater than unity. This means that in the space filled with the gain medium, only one counter-wave propagates, which emerges from infinity and carries energy toward the incident wave, which obviously contradicts the causality principle.

This solution came under criticism in [41], where it was pointed out that waves appearing "during successive reflections from layer boundaries form, for large enough d, a divergent series, and the solution is simply absent." In fact, this corresponds to the divergence of a series of Airy partial waves [88, 89]. Obviously, we have a contradiction between the finite result obtained by the Fresnel method and the divergence of the Airy series. We note that the result of summation of the Airy series for dissipative media always agrees with predictions of the Fresnel approach.

To resolve this paradox, the author of [41] proposed considering the propagation of a pulse instead of a stationary problem of the propagation of an infinite plane wave. It was asserted that if the pulse amplitude inside the layer increases infinitely with time, then the Fourier transform of the field amplitude $E(z,\omega)$ does not exist. Therefore, the field representation as a sum of monochromatic waves is also invalid in this case. Instead, it was proposed that the field be expanded in waves with exponentially increasing amplitudes (see also [90]), in accordance with the generalized Fourier

transformation [91, 92]. In this case, the integration contour in the complex frequency plane in the inverse Fourier transformation is located above all poles of the integrand. We show below that the poles lying above the real axis give a correction to the standard solution obtained by the Fresnel method, which exponentially increases with time.

In the next section, we consider an electromagnetic wave in the form of a semi-infinite train with a finite leading edge propagating through a gain layer, and compare the results obtained by the Fresnel and Airy methods and the numerical solution of Maxwell–Bloch equations obtained by the FDTM method.

3.2 Fresnel and Airy approaches

We consider the problem of the normal incidence of a semi-infinite sinusoidal train with a smooth wave front on a gain layer with thickness d. We assume for definiteness that the train is incident from left to right. Assuming that condition (2c) is satisfied, we neglect the nonlinearity at the first stage, i.e., we use the dielectric constant of type (2d) in Eqn (2a). The linearity of the problem allows passing to the Fourier representation for the amplitude $E(z,t)$. In this case, the analysis reduces to the problem of the propagation of a plane wave through a homogeneous layer with a negative imaginary part of the dielectric constant $\operatorname{Im}\varepsilon_{\text{gain}} < 0$, when the distribution of the field $E(z,\omega)$ is represented as the product of the field distribution $g(z,\omega)$ for a single incident wave and the incident wave amplitude. The form of the function $g(z,\omega)$ is found by solving ordinary second-order differential equation (2a) using Maxwell's boundary conditions for the continuity of the fields (Fresnel approach):

$$g(z,\omega) = \begin{cases} \exp(\mathrm{i}k_0 z) + r(d)\exp(-\mathrm{i}k_0 z), & z < 0, \\ a(d)\exp\left(\mathrm{i}k_0 z\sqrt{\varepsilon_{\text{gain}}}\right) + b(d)\exp\left(-\mathrm{i}k_0 z\sqrt{\varepsilon_{\text{gain}}}\right), & 0 < z < d, \\ t(d)\exp\left(\mathrm{i}k_0(z-d)\right), & z > d. \end{cases} \tag{3a}$$

The amplitudes $r(d)$, $a(d)$, $b(d)$, and $t(d)$ are found by matching the tangential components of the fields at the boundaries of layers $z = 0$ and $z = d$ [58]:

$$r(d) = -\frac{(Z_1^2 - Z_2^2)\left(\exp\left(-\mathrm{i}k_0 d\sqrt{\varepsilon_{\text{gain}}}\right) - \exp\left(\mathrm{i}k_0 d\sqrt{\varepsilon_{\text{gain}}}\right)\right)}{(Z_1+Z_2)^2\exp\left(-\mathrm{i}k_0 d\sqrt{\varepsilon_{\text{gain}}}\right) - (Z_1-Z_2)^2\exp\left(\mathrm{i}k_0 d\sqrt{\varepsilon_{\text{gain}}}\right)},$$

$$t(d) = \frac{4Z_1 Z_2}{(Z_1+Z_2)^2\exp\left(-\mathrm{i}k_0 d\sqrt{\varepsilon_{\text{gain}}}\right) - (Z_1-Z_2)^2\exp\left(\mathrm{i}k_0 d\sqrt{\varepsilon_{\text{gain}}}\right)},$$

$$a(d) = \frac{2Z_2(Z_1+Z_2)\exp\left(-\mathrm{i}k_0 d\sqrt{\varepsilon_{\text{gain}}}\right)}{(Z_1+Z_2)^2\exp\left(-\mathrm{i}k_0 d\sqrt{\varepsilon_{\text{gain}}}\right) - (Z_1-Z_2)^2\exp\left(\mathrm{i}k_0 d\sqrt{\varepsilon_{\text{gain}}}\right)},$$

$$b(d) = \frac{2Z_2(Z_1-Z_2)\exp\left(\mathrm{i}k_0 d\sqrt{\varepsilon_{\text{gain}}}\right)}{(Z_1+Z_2)^2\exp\left(-\mathrm{i}k_0 d\sqrt{\varepsilon_{\text{gain}}}\right) - (Z_1-Z_2)^2\exp\left(\mathrm{i}k_0 d\sqrt{\varepsilon_{\text{gain}}}\right)}, \tag{3b}$$

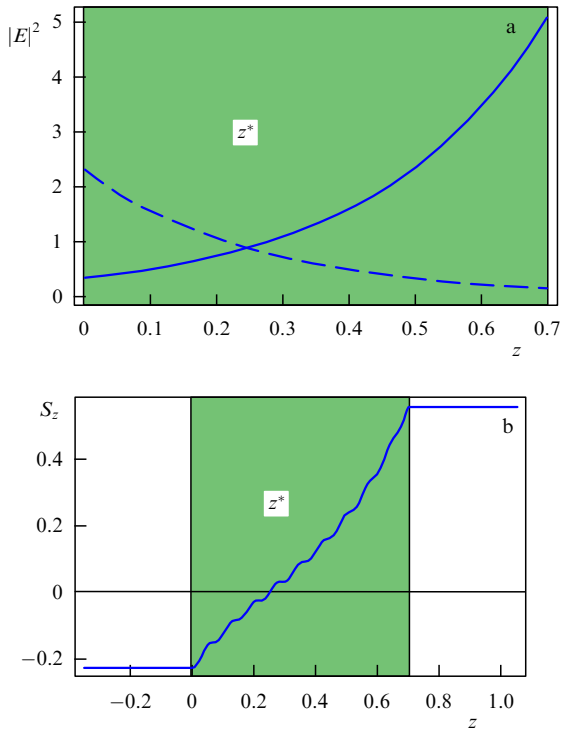

Figure 1. (See in color online.) Calculations of the electric field $E(z,\omega)$ by the Fresnel method. (a) Incident (solid curve) and counter (dashed curve) waves. (b) Energy flux S_z in a layer with a thickness $d > d_0$. The gain layer is shaded. The incident wave frequency ω is equal to the QD transition frequency ω_0; the dielectric constant $\varepsilon_{\text{gain}} = 2 - 0.182\mathrm{i}$ is obtained from expression (2d) for the values of parameters typical for gain media with semiconductor QDs [24].

where $Z_1 = 1$ and $Z_2 = 1/\sqrt{\varepsilon_{\text{gain}}}$ are characteristic impedances of the vacuum and the medium and k_0 is the wave number in the vacuum. We note that the wave field in the layer is the sum of the fields of two waves (Fig. 1). One of them, with a positive real part of the wave number and a positive z component of the Poynting vector, increases (is amplified), penetrating into the layer. We call this wave the 'incident' wave, and the second wave, the 'counter' wave. The counter wave decreases in the depth of the layer and has a negative component S_z of the Poynting vector. The ratio of the electric field strengths on the right boundary $z = d$ of the layer is uniquely defined by the impedance of the transmitted wave, and is therefore independent of the layer thickness. Because the counter wave (dashed curve in Fig. 1a) traveling from right to left is amplified, its strength for a large enough layer thickness at the left boundary $z = 0$ exceeds the incident wave strength (solid curve in Fig. 1a).[1] The $z = z^*$ plane, determined by the equality of the field strengths of the forward and backward waves, is also characterized by the zero energy flux propagating through this plane. For $z < z^*$, the energy flux is directed to the left, and for $z > z^*$, to the

[1] In all numerical calculations, we use parameters typical for amplifying media with semiconductor QDs [24]: $\omega_0 = 10^{15}\ \text{s}^{-1}$, $\tau_{\text{P}} = 3\times10^{-14}$ s, $\tau_n = 5\times10^{-13}$ s, $n_0 = 2.15\times10^{18}$ atom cm^{-3}, $|\mu|^2 = (1.5\times10^{-17})^2$ dyn cm^3, $\varepsilon_0 = 2$ in the gain layer ($0 < z < d$), and $\varepsilon_0 = 1$ outside the layer. Further, for the convenience of comparing, system (1) is transformed into a dimensionless one in which the time $(t, \tau_{\text{P}}, \tau_n)$ was measured in units of τ_{P}, the coordinate in units of $c\tau_{\text{P}}$, frequency ω_0 in units of τ_{P}^{-1}, E and P in units of $\sqrt{\hbar n_0/\tau_{\text{P}}}$, n in units of n_0, and $|\mu|^2$ in units $\hbar/(n_0\tau_{\text{P}})$. As a result, we obtain the values of dimensionless parameters $\omega_0 = 30$, $\tau_{\text{P}} = 1$, $\tau_n = 167$, $n_0 = 1$, and $|\mu|^2 = 0.0145$; in this case, the constants c and $\hbar$ disappear from the equations.

right. The distance d_0 from the $z = z^*$ plane to the right boundary of the layer can be readily obtained from Eqns (3b) and the condition that the intensities of counterpropagating waves in the plate be equal. Hence,

$$d_0 = \frac{1}{4k_0\kappa} \ln\left[\frac{(n_{\text{gain}}+1)^2 + \kappa_{\text{gain}}^2}{(n_{\text{gain}}-1)^2 + \kappa_{\text{gain}}^2}\right], \tag{4}$$

where $n_{\text{gain}} = \operatorname{Re}\sqrt{\varepsilon_{\text{gain}}}$ and $\kappa_{\text{gain}} = \operatorname{Im}\sqrt{\varepsilon_{\text{gain}}}$. We note that d_0 depends on the pumping level κ_{gain}, and can be for the same sample either larger or smaller than its thickness d.

Expression (4) for d_0 is approximate and was found from the condition of the equality of intensities of the waves in a plate. But this condition does not guarantee the zero energy flux:

$$S_z = \frac{c}{4\pi}\Big[n_{\text{gain}}\big(a(d_0)\,a^*(d_0) - b(d_0)\,b^*(d_0)\big) + 2\kappa_{\text{gain}}\operatorname{Im}\big(a(d_0)\,b^*(d_0)\big)\Big].$$

We see from this expression that for a nonzero imaginary part of the wave number, $\operatorname{Im} k = \kappa_{\text{gain}}$, counterpropagating waves in the presence of a phase difference between them make an interference contribution to the energy flux [71]. The interference correction is manifested as a fine ripple in Fig. 1b, which somewhat shifts the point where $S_z = 0$. However this influence is typically insignificant.

As noted above, if the layer thickness exceeds d_0, a region appears inside the layer where the energy flux is directed toward the incident wave (Fig. 1b). It follows from the continuity of the energy flux inside the layer and its constant value outside the layer that for $d > d_0$, the reflection coefficient exceeds unity. As the layer thickness is further increased, the Fresnel approach predicts an increase in the region where the counterpropagating wave dominates, which decreases from left to right and transfers energy from right to left, toward the incident wave [42]. The energy is transferred from left to right only in a thickness-d_0 layer adjacent to the rear boundary of the layer. It is important to note that the Fresnel approach in (3b) predicts that the transmission coefficient T tends to zero and the reflection coefficient R tends to a finite value as the layer thickness increases (Fig. 2). Thus, the passage to the limit of a half-space ($d/d_0 \to \infty$) gives a reflection coefficient greater than unity and a counter propagating wave in the half-space (see [42]).

In the case of dissipative media, the field distribution calculated by the Fresnel method, Eqn (3), coincides with that calculated by the summation of partial Airy waves appearing during successive reflections of waves from the layer boundaries [93, 94]. In the case of a gain layer, the results obtained by the Airy and Fresnel methods can be different. We consider the Airy procedure (Fig. 3) in more detail. The incident wave with the unit amplitude is scattered by the front surface of a sample. As a result, a reflected wave with the amplitude

$$r_\infty = \frac{Z_1 - Z_2}{Z_1 + Z_2} \tag{4a}$$

and a transmitted wave with the amplitude $t_{\infty 1} = 2Z_1/(Z_1 + Z_2)$ appear, where r_∞ and $t_{\infty 1}$ are the reflection and transmission coefficients in the problem in the half-space. It is usually assumed that the transmitted wave is incident [41], i.e., $\operatorname{Re} Z_2 > 0$. This wave propagates in the sample and

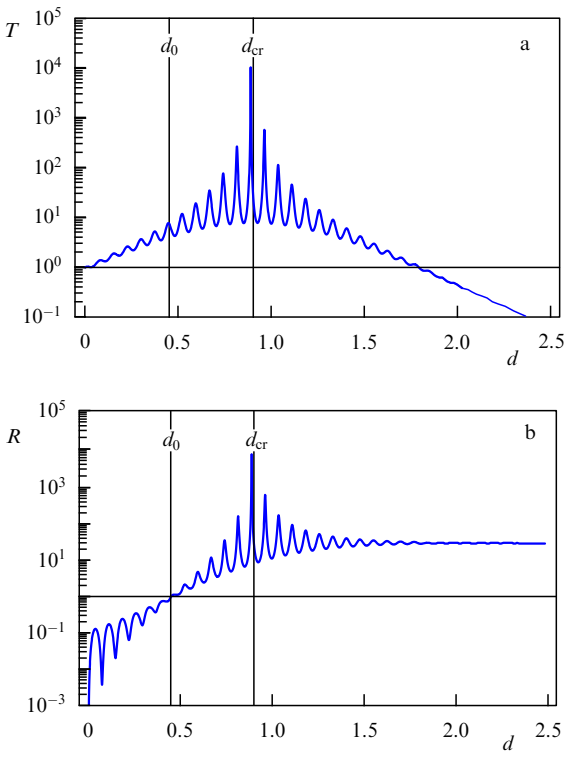

Figure 2. (See in color online.) (a) Transmission and (b) reflection coefficients T and R (in terms of intensity) of a gain layer calculated as functions of the layer thickness d by the Fresnel method. The parameters are the same as in Fig. 1.

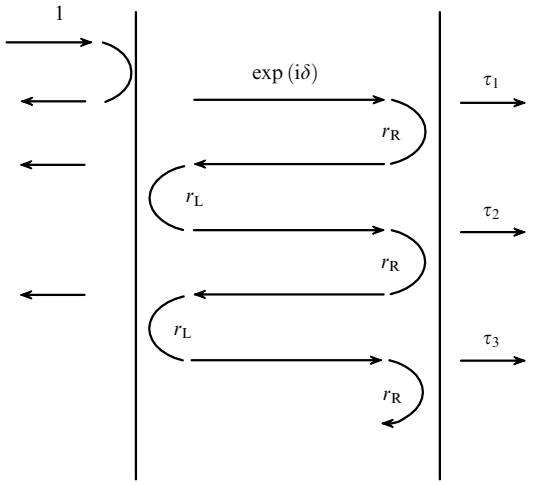

Figure 3. Airy's procedure for calculating reflection and transmission coefficients of a plate as successive rereflections. For a homogeneous layer, $r_{\text{L}} = r_{\text{R}} = -r_\infty$.

its amplitude on the right boundary ($z = d$) acquires the factor $\exp(\mathrm{i}\delta)$, $\delta = k_0 d\sqrt{\varepsilon_{\text{gain}}}$. Then the wave passes through the right boundary with the coefficient $t_{\infty 2} = 2Z_2/(Z_1 + Z_2)$, such that the amplitude of the first wave transmitted through the sample is

$$\tau_1 = t_{\infty 1} t_{\infty 2} \exp\left(\mathrm{i}k_0 d\sqrt{\varepsilon_{\text{gain}}}\right).$$

A part of the wave is reflected from the right boundary of the sample with the reflection coefficient $-r_\infty$, transforming into

a counter wave. Then the wave propagates in the sample from right to left, is reflected from the left boundary with the reflection coefficient $-r_\infty$, transforms into an incident wave, and propagates from left to right up to the sample boundary. During the propagation of this incident wave through the boundary, a second transmitted partial wave with the amplitude $\tau_2 = \tau_1 q$ appears, where

$$q = r_\infty^2 \exp\left(2ik_0 d\sqrt{\varepsilon_{\text{gain}}}\right) = r_\infty^2 \exp\left(2i\delta\right). \tag{4b}$$

The amplitude of each subsequent partial wave is obtained by multiplying by the factor q (the denominator of a geometric progression). As a result, the total transmission coefficient is given by the series

$$t(d) = t_{\infty 1} t_{\infty 2} \exp\left(ik_0 d\sqrt{\varepsilon_{\text{gain}}}\right)\left(1 + r_\infty^2 \exp\left(2i\delta\right) + \ldots\right)$$

$$= t_{\infty 1} t_{\infty 2} \exp\left(ik_0 d\sqrt{\varepsilon_{\text{gain}}}\right) \sum_{n=0}^{\infty} \left(r_\infty^2 \exp\left(2i\delta\right)\right)^n. \tag{5}$$

Summing geometric series (5) gives (3b).

We note that series (5) converges only for $|q| < 1$. This condition corresponds either to the absence of gain or, in its presence, to a small thickness of the layer $d < d_{\text{cr}}$. For $d = d_{\text{cr}}$, the modulus of q becomes unity. For $d < d_{\text{cr}}$, the attenuation of the wave due to its escape from the sample exceeds its gain during the passage of the wave in the gain medium. The value of d_{cr} is exactly twice as large as the value of d_0 and is given by

$$d_{\text{cr}} = 2d_0 = \frac{1}{2k_0\kappa_{\text{gain}}} \ln\left[\frac{(n_{\text{gain}}+1)^2 + \kappa_{\text{gain}}^2}{(n_{\text{gain}}-1)^2 + \kappa_{\text{gain}}^2}\right]. \tag{6a}$$

For $d > d_{\text{cr}}$, Airy series (5) diverges, while Fresnel approach (3) gives a finite amplitude of the transmitted wave.

Hence, for $d > d_{\text{cr}}$, the Fresnel and Airy approaches give different results. For this reason, we performed a numerical FDTD modeling of the solution of Maxwell–Bloch equations (1) correctly describing the gain medium. We considered the temporal problem of the normal incidence of a semi-infinite wave train with a smooth leading edge on a gain layer. For comparison with the Fresnel and Airy approaches, we calculated the stationary field distribution appearing after the end of the transient process.

We can see from Fig. 4a that in the region of parameter values for which Airy series (5) converges ($d < d_{\text{cr}}$), the results of both analytic approaches agree with numerical calculations. For thicknesses $d_{\text{cr}} < d < d_{\text{las}}$, Airy series (5) diverges, but the Fresnel approach and numerical simulations give the same results (Fig. 4b). For thicknesses exceeding some value d_{las}, lasing begins to develop, and field strengths obtained in numerical experiments begin to exceed the field strength obtained by the Fresnel method (Fig. 4c). This is caused by the violation of condition (2c), and the established solution cannot be described in the linear approximation, i.e., by using the Fresnel approach.[2]

The construction of Airy series (5) quite visually describes the propagation of a semi-infinite wave train through a layer of matter. However, in the case of a gain medium, it should be performed differently for $d < d_{\text{cr}}$ and $d > d_{\text{cr}}$. Indeed, r_∞ in (5) is the reflection coefficient in the problem of reflection of a plane wave from a half-space. The value of r_∞ depends on the wave in the layer with which the wave incident from the vacuum is matched.

[2] The region of d values near d_{cr} is considered below.

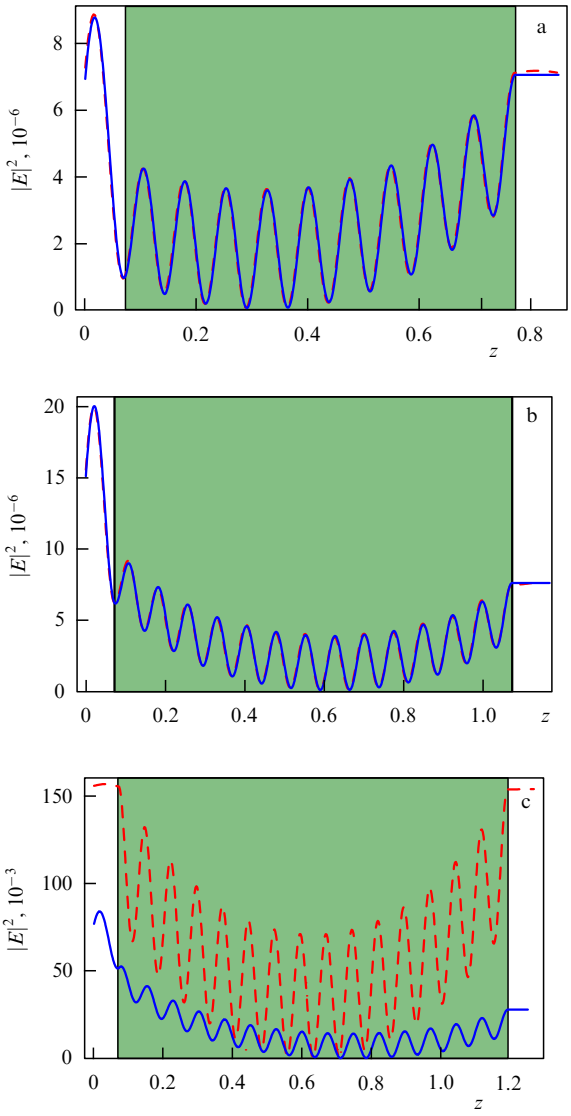

Figure 4. (See in color online.) Electric field intensity calculated by the Fresnel method (3) (solid curves) and from Maxwell–Bloch equations (1) (dashed curves) for a wave propagating (a) through a layer with the thickness $d = 0.7$ smaller than the critical value $d_{\text{cr}} \approx 0.905$, (b) through a layer with the thickness $d = 1$ greater than the critical value, when lasing is still absent, and (c) through a layer with the thickness $d = 1.12$, when lasing appears. The incident wave frequency ω is equal to the QD transition frequency ω_0. The dipole moment of the QD is $|\mu|^2 = 0.0145$, the incident wave intensity is (a) 10^{-6}, (b) 10^{-6}, and (c) 10^{-3} in dimensionless units (see footnote 1).

If, as is usually accepted for dissipative media [95], we take a wave transferring energy inside a layer, then for $d < d_{\text{cr}}$, the modulus of the denominator of the geometric progression $q = r_\infty^2 \exp\left(2i\delta\right)$, where $\delta = k_0 d\sqrt{\varepsilon_{\text{gain}}}$, is smaller than unity, $|q| < 1$, and the Airy series in incident waves converges to expression (3b) obtained by the Fresnel method. But if we assume in the Airy procedure that a solution in a semi-infinite medium is a counterpropagating wave [42] transferring energy to the boundary $z = 0$ from infinity, then the impedance Z_2 and complex phase δ change their signs. As a result, the denominator of progression (5) becomes equal to $1/q$. This means formally that for $d > d_{\text{cr}}$, the Airy series in counterpropagating waves converges, as it does in the Fresnel calculations (3b).

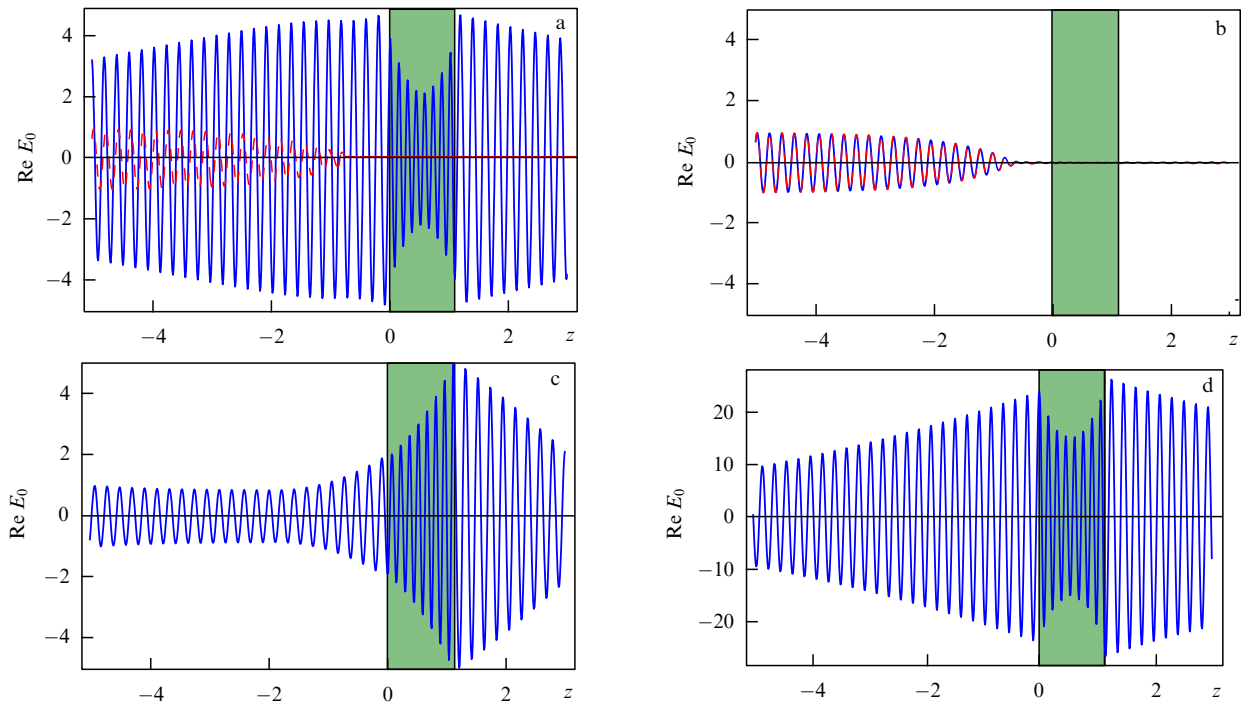

Figure 5. (See in color online.) Electric field distributions in a wave train incident on a gain layer calculated by different methods. (a) The Fresnel approach. The instant $t = 0$ when the leading edge of the train has not reached the layer. The solid curve shows the field distribution found from (8), the dashed curve shows the real field distribution in the train; (b) the same calculated by the modified Fresnel approach; (c) amplification of the train field (modified Fresnel calculation) for $t = 5.5$; (d) the train field at a later instant $t = 15.5$ coming to a localized eigenstate with a complex frequency. Parameters are the same as in Fig. 1.

Analysis shows that result (3b) obtained by the Fresnel method can be regarded as an analytic continuation of the sum of Airy series (5) to the region $d > d_{\rm cr}(\omega)$ in the complex frequency plane. In other words, for $d < d_{\rm cr}$, the Airy series in incident waves should be used, and for $d > d_{\rm cr}$, the Airy series in counterpropagating waves should be used. We recall that for $d = d_{\rm cr}$ $(|q| = 1)$, neither of these series converges. If $q \neq 1$, the limit $d \to d_{\rm cr} + 0$ of the sum of series (5) in counterpropagating waves coincides with the limit $d \to d_{\rm cr} - 0$ of the sum of series (5) in incident waves. We recall that lasing is still absent. The use of the series in counterpropagating waves is equivalent to the continuation of the function $1/(1-q)$ beyond its convergence radius. Indeed [56],

$$\frac{1}{1-q} = -\frac{1/q}{1-1/q} = -\frac{1}{q}\sum_{n=0}^{\infty}\left(\frac{1}{q}\right)^n . \tag{6b}$$

Thus, we obtain complete correspondence between Airy series and the result of the Fresnel approach in all cases considered here.

3.3 Temporal problem of the propagation of a semi-infinite wave train through a gain layer

To find the reason for the discrepancy between the seemingly reliable Fresnel approach (Fig. 4c) and the numerical solution of the Maxwell–Bloch system, we consider the temporal problem of the propagation of a semi-infinite wave train through a gain layer. We assume that the leading edge of the train $E_0(z,t)$ reaches the point $z = 0$ at the instant $t = 0$, and the train shape is

$$E_0(z=0,t) = \begin{cases} 0\,, & t < 0\,, \\ \left(1 - \exp\left(-\dfrac{t}{\sigma}\right)\right)\exp\left(-\mathrm{i}\Omega t\right), & t > 0\,, \end{cases}$$

where Ω is the carrier frequency of the train and σ is the leading edge width.

To correctly find the spectrum of such a pulse,

$$e_0(\omega) = (2\pi)^{-1}\int_{-\infty}^{\infty} E_0(t)\exp\left(\mathrm{i}\omega t\right)\mathrm{d}t\,, \tag{7a}$$

a certain accuracy is required [96], because $E_0(z=0,t)$ is not a compact function (it does not decrease as $t \to +\infty$). Here, we can use the standard procedure [92] of finding the spectrum of the product $E_0(z=0,t)\exp\left(-\gamma t\right)$ and then sending γ to zero. As a result, the expression

$$e_0(\omega) = -\frac{1}{2\pi\sigma(\omega-\Omega)(\omega-\Omega+\mathrm{i}/\sigma)} \tag{7b}$$

is obtained.

In the absence of the layer, according to linear Helmholtz equations (2a), (2d), each harmonic $e_0(\omega)\exp\left(-\mathrm{i}\omega t\right)$ of the field specified at the point $z = 0$ produces a plane wave $e_0(\omega)\exp\left(-\mathrm{i}\omega t\right)\exp\left(\mathrm{i}\omega z/c\right)$ in the entire space, which propagates to the right. The sum of these plane waves,

$$\begin{aligned} E_0(z,t) &= \int_{-\infty}^{\infty} e_0(\omega)\exp\left(-\mathrm{i}\omega t\right)\exp\left(\frac{\mathrm{i}\omega z}{c}\right)\mathrm{d}\omega \\ &= \int_{-\infty}^{\infty} e_0(\omega)\exp\left(-\mathrm{i}\omega\left(t-\frac{z}{c}\right)\right)\mathrm{d}\omega = E_0\left(0, t-\frac{z}{c}\right), \end{aligned}$$

is equal to the train field propagating with time to the right without changing its shape (the dashed curve in Fig. 5a). We note that $E_0(z,t) = 0$ for $z/c > t$, in accordance with the causality principle.

In the presence of a layer located in the region $z \notin [0,d]$, the total (incident plus scattered) field of the train should also

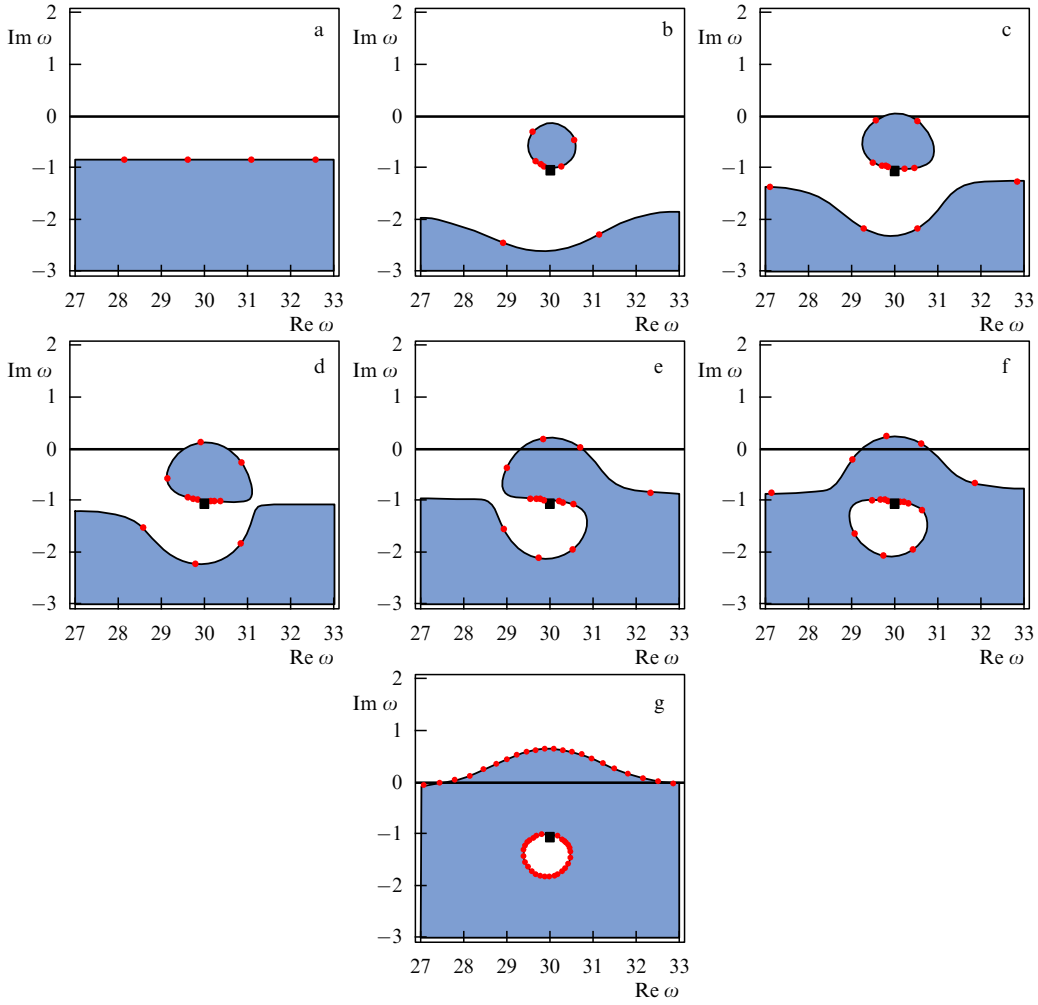

Figure 6. (See in color online.) Poles of the response function $g(z,\omega)$ (indicated by circles) and a pole of the dielectric constant (indicated by a square). Regions $d > d_{\rm cr} \approx 0.905$ are shaded; (a) quantum dots are absent ($|\mu|^2 = 0$), the layer thickness is $d = 1.5$; (b–g) quantum dots are present, $|\mu|^2 = 0.0145$, layer thickness is (b) $d = 0.7$, (c) 1.0, (d) 1.12, (e) 1.5, (f) 2.0, (g) 7.0. The parameters are the same as in Fig. 1.

obey the causality principle, i.e., the scattered wave should be absent until the train front reaches the left boundary $z = 0$ of the layer. For $t < 0$, the total field should be equal to $E_0(0, t - z/c)$.

The Fourier harmonic of the total field in the presence of the layer is equal to the incident harmonic amplitude $e_0(\omega)$ times the transfer function $g(z,\omega)$ in (3a). We recall that this function was found using the Fresnel approach. It describes the field distribution in the vacuum–layer–vacuum system in the case of normal incidence of a plane wave with the unit amplitude. In this case, the time dependence of the field is found by the inverse Fourier transformation

$$E(z,t) = \int_{-\infty}^{\infty} e_0(\omega)\, g(z,\omega) \exp(-\mathrm{i}\omega t)\, \mathrm{d}\omega\,. \tag{8}$$

In the case of a dissipative layer or a gain layer with a thickness $d < d_{\rm cr}$, this procedure gives the correct shape of the initial pulse, $E(z,t) = E_0(0, t - z/c)$. But for $d > d_{\rm las} \geqslant d_{\rm cr}$, where $d_{\rm las}$ is the thickness at which lasing begins, a different field distribution is obtained (the solid curve in Fig. 5a). We can see from Fig. 5a that the scattered wave appears before the leading edge of the train reaches the layer, i.e., the causality principle is obviously violated. This violation indicates that the Fresnel approach should be modified.

It is known that the causality principle determines the analytic properties of the transfer function $g(z,\omega)$ (which is by its nature a response function) as a function of the complex frequency ω [58]. The function $g(z,\omega)$ has singularities in the form of poles in the ω plane at the points $\omega_j = \mathrm{Re}\,\omega_j + \mathrm{i}\,\mathrm{Im}\,\omega_j$, $j = 1, 2, \ldots$, corresponding to the eigenmodes of the layer as an open resonator [97, 98]. The positions of poles in the ω plane are determined from the condition of vanishing denominators, which are the same for all field amplitudes (3b):

$$\left(\frac{\sqrt{\varepsilon_{\rm gain}(\omega)} - 1}{\sqrt{\varepsilon_{\rm gain}(\omega)} + 1}\right)^2 \exp\left(2\mathrm{i}\,\frac{\omega}{c}\, d\sqrt{\varepsilon_{\rm gain}(\omega)}\right) = 1\,, \tag{9}$$

which is equivalent to the condition $q = 1$.

In the absence of gain (in a dissipative layer), all poles of $g(z,\omega)$ are located in the lower half-plane of the complex frequency ω (Fig. 6a). In this case, inverse Fourier transformation (8) gives the physically meaningful result.

In the case of a gain layer, according to (9), additional poles occur (Fig. 6b), which pass to the upper half-plane of the complex frequency ω with increasing pumping [the

parameter α in (2b)] (Fig. 6d), which first occurs at $d = d_{las}(\alpha)$. As a rule, the line $|q| = 1$ touches the axis $\mathrm{Im}\,\omega = 0$ at $d = d_{cr} < d_{las}$. In the case $d_{cr} < d < d_{las}$, a range of real frequencies exists where the Airy series diverges, but lasing is absent (Fig. 6c), and therefore the Airy series in counterpropagating waves and calculations using Fresnel formulas give the correct result.

If the inverse Fourier transformation is performed in the usual way (8) [58], the appearance of poles in the upper half-plane leads to the violation of the causality principle. In this case, expression (8) should be modified [41, 90], taking into account that the transfer function $g(z, \omega)$ is a response function by its nature. To obtain the time representation of the response function

$$G(z, t) = (2\pi)^{-1} \int_C g(z, \omega) \exp(-\mathrm{i}\omega t)\, \mathrm{d}\omega$$

satisfying the causality principle [$G(z, t) = 0$ for $t < 0$], the integration contour C in the inverse Fourier transformation

$$E(z, t) = \int_C e_0(\omega)\, g(z, \omega) \exp(-\mathrm{i}\omega t)\, \mathrm{d}\omega \qquad (10)$$

must be drawn above all existing poles. It can then be deformed such that expression (10) takes the form of the sum of the integral along the real axis and all residues at the poles [41, 90]:

$$E(z, t) = \int_{-\infty}^{\infty} e_0(\omega)\, g(z, \omega) \exp(-\mathrm{i}\omega t)\, \mathrm{d}\omega - 2\pi\mathrm{i} \sum_j \mathrm{res}\left[g(\omega_j, z)\right] e_0(\omega_j) \exp(-\mathrm{i}\omega_j t)\,. \qquad (11)$$

We note that the integral along the real ω axis in expression (11) coincides with the result obtained in the standard Fresnel approach (8). As we saw above (Fig. 5a), the first term in (11) by itself leads to a violation of the causality principle. Integration over the new contour adds residues at a discrete set of frequencies ω_j in the form of terms $\sim \exp(-\mathrm{i}\,\mathrm{Re}\,\omega_j t) \exp(\mathrm{Im}\,\omega_j t)$ increasing with time [41, 90, 99]. Adding these discrete modes makes the calculation scheme consistent with the causality principle, i.e., the reflected wave is absent until the train front reaches the layer boundary (Fig. 5b). Below, we call the above calculation of the wave field taking discrete modes into account the modified Fresnel approach.

Each eigensolution in (11) appearing at the frequency of one of the poles represents a field exponentially increasing with time in the layer and exponentially decreasing with the distance from it (Fig. 5d) [41, 90, 99]. This decrease occurs because the imaginary part of the wave number is positive outside the gain layer, $\mathrm{Im}\,(\omega/c) > 0$. Therefore, the neglect of the contribution from the discrete spectrum of poles in (11) is a source of errors appearing in the Fresnel approach. It is the correct account of the contribution from these poles that ensures the causality principle in the analysis of this problem.

Because the modified Fresnel approach was obtained from linearized Maxwell–Bloch equations, it quite correctly describes the behavior of the field at the linear stage of lasing development, when the field satisfies smallness criterion (2c) (Fig. 7). However, the field infinitely increases with time. In this case, not the reflected wave, as predicted by calculations in the framework of the standard Fresnel approach [42], but the wave transmitted through the layer is mainly amplified (Fig. 5c). However, stationary field strengths can be obtained only using the nonlinear approach.

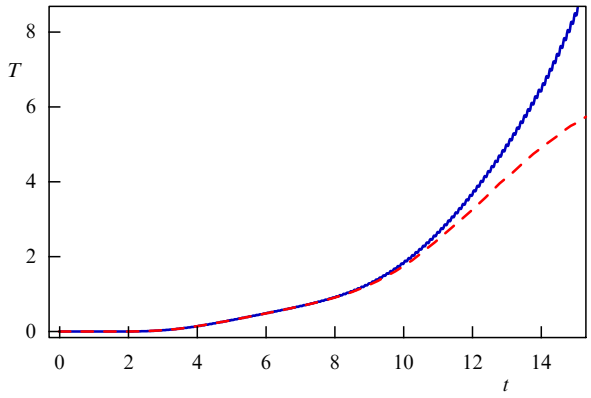

Figure 7. Time dependences of the transmission coefficient calculated by the Fresnel method (solid curve) and by solving Maxwell–Bloch equations numerically (dashed curve) for a semi-infinite sinusoidal wave train incident on a gain layer. The incident wave intensity is 10^{-6} in dimensionless units (see footnote 1).

It is important to note the relation between the poles of the response function and the critical layer thickness. The position of the poles is determined by Eqn (9), while critical length (6a) is determined by the violation of the convergence condition for the Airy series, i.e., in fact by the same equality (9), but taken by modulus. Therefore, all the poles lie on curves defined by the condition $d = d_{cr}(\omega)$, where ω takes complex values (see Fig. 6). For a sufficiently thick layer [or sufficiently strong pumping, determined by the coefficient α in (2d)], a region where $d > d_{cr}(\omega)$ appears on the real frequency axis. In this region, the Airy series no longer converges (the intersection of the shaded region with the abscissa in Fig. 6c), but Fresnel approach (8) still gives a result coinciding with the numerical solution of Eqns (1) (Fig. 6c). Lasing appears for a somewhat larger thickness d_{las} of the layer (or a higher pumping level), when one of the poles passes to the upper half-plane (Fig. 6d), and only in this case does the Fresnel approach give an incorrect result. Therefore, the divergence condition for the Airy series is necessary, but insufficient for the onset of lasing, and can be used only as an approximate estimate of the condition for lasing appearance.

An interesting feature of the problem is the motion of poles in the complex plane with increasing the layer thickness. The poles move along the curve $d = d_{cr}(\omega)$, and they can come out to the upper half-plane and return to the lower half-plane. As a result, as d increases, lasing alternately appears and disappears. Therefore, a set of thicknesses d_{las} with a maximum value d_{th} can exist. For thicknesses larger than d_{th}, at least one pole is in the upper half-plane, and after that lasing no longer disappears with increasing the layer thickness.

As pointed out above, as long as lasing is absent, the standard Fresnel approach gives the same result as the solution of nonlinear Maxwell–Bloch equations. This statement is illustrated in Fig. 8a, where the dependence of the stationary transmission coefficient T on the layer thickness at a fixed frequency is shown. We see that the field distribution obtained by solving Maxwell–Bloch equations deviates from

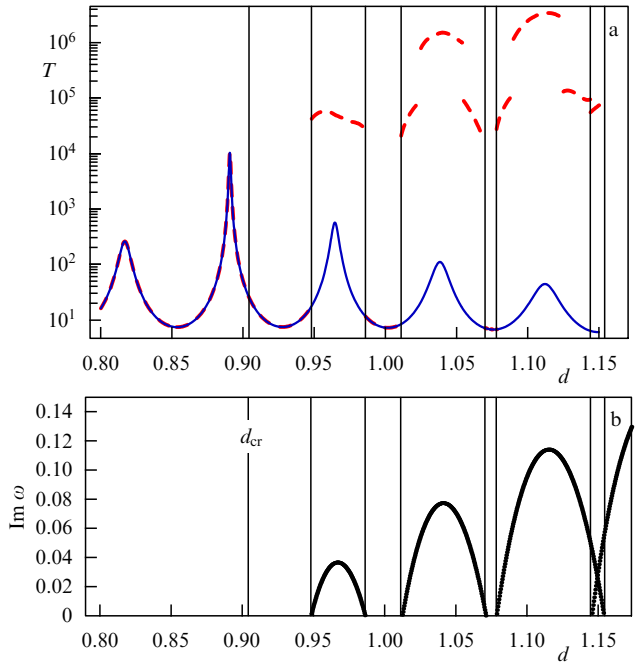

Figure 8. (See in color online.) (a) Transmission coefficient of a layer calculated by the Fresnel method (solid curve) and by solving Maxwell–Bloch equations numerically (dashed curve) as a function of the layer thickness. (b) Positions of poles with $\mathrm{Im}\,\omega > 0$ as functions of the layer thickness. The incident wave intensity is 10^{-6}.

the standard Fresnel field distribution[3] at the values of d when bands appear in the upper complex frequency half-plane.

We note that at frequencies different from the lasing frequency, the Fresnel approach predicts a smooth change in the stationary intensity of the transmitted wave with the layer thickness. For some layer thicknesses, intensity maxima of the transmitted wave are observed (Fig. 8a). But nonlinear Maxwell–Bloch equations predict intensity jumps in this dependence (Fig. 8a) even in the case of an infinitely small incident wave intensity. These jumps are observed, however, not for layer thicknesses where intensity peaks are located but for layer thicknesses at which lasing starts or terminates. At this point, a pole either comes out to the upper complex frequency half-plane (lasing begins) or passes to the lower half-plane (lasing ceases).

At incident wave frequencies close to the laser frequency, the Fresnel approach gives an infinite field strength when approaching d_{las}. However, nonlinear Maxwell–Bloch equations predict a finite field strength, with the dependence of the transmitted wave intensity on the sample thickness in the nonlinear lasing regime having an evident hysteresis character (Fig. 9), which is related to the layer bistability in the lasing mode (the physics of this phenomenon is most simply described by the field-mode–two-level-atom model [78]).

At the incident wave frequency different from the lasing frequency, the possibility of the onset of lasing and transition to the nonlinear mode is related to the presence of the leading edge of the incident wave train, which contains all the frequency harmonics. The control of the carrier wave

[3] We note that violation of the convergence condition for the Airy series does not always lead to a deviation of the real field distribution from the Fresnel distribution.

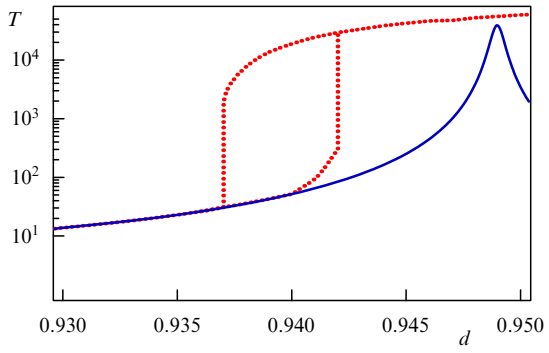

Figure 9. Transmission coefficient of a gain layer for an electromagnetic wave as a function of the layer thickness. The incident wave intensity is 10^{-2}.

amplitude gives the coincidence with the Fresnel approach up to the thickness d_{las} and the subsequent intensity jump (Fig. 8b) after exceeding this thickness.

4. Lasing in photonic crystals

We have considered the propagation of light through a single gain layer. We now consider the propagation of light through a finite multilayer system in which gain layers alternate with 'normal' layers. Such a system is also called a one-dimensional photonic crystal (PC). The problem of the incidence of a wave on a PC has some features related first of all to the presence of allowed and forbidden bands determining the behavior of the field at the scale of a few unit cells of the PC. The field intensity distribution also changes within one cell because the field energy concentrates in certain regions of a PC cell depending on frequency (Borrmann effect [74]), and the field intensity in gain layers can exceed the field intensity in a single layer for the same amplitudes of incident waves. In addition, the PC band structure itself changes in the presence of pumping because of the change in the frequency dispersion of the dielectric constant $\varepsilon_{gain}(\omega)$. These features are manifested already in the simplest case where the PC consists of a sequence of gain layers separated by vacuum layers with respective thicknesses d_1 and d_2 and dielectric constants $\varepsilon_{gain}(\omega)$ ($\mathrm{Im}\,\varepsilon_{gain}(\omega) < 0$) and $\varepsilon_2 = 1$.

The simplest method for calculating the transmission and reflection coefficients of PCs is the T-matrix method [95]. As applied to PCs, the T-matrix method is equivalent to the Fresnel approach for a homogeneous layer. The Airy approach can also be generalized by replacing plane waves by Bloch waves.

If the thickness of a gain PC is sufficiently large, lasing can develop in it. In this review, we consider only the linear stage of the propagation of waves in a PC, because we are mainly interested in subthreshold phenomena. At present, the nonlinear optics of PCs is a rapidly developing field, and the results of investigations in this field are considered, e.g., in [84, 100, 101].

4.1 Airy series for photonic crystals

In Section 3.2, we analyzed the details of the Airy approach for a single homogeneous layer, when the propagation of a wave is considered as a sequence of rereflections inside the layer. We generalize this method to the case of an arbitrary number of layers. There are two eigensolutions for a PC, the Bloch waves $E^{\pm} = f^{\pm}(z)\exp(\pm ik_B z)$. To construct the Airy

series in Bloch waves, it suffices to know the Bloch wave number k_B and impedances $Z^{\pm}$ (or admittances $\zeta^{\pm} = 1/Z^{\pm}$) of these waves.[4] We note that, unlike the Bloch wave number k_B defined up to the reciprocal lattice vector, the wave impedance $Z^{\pm}$ at a given point is uniquely defined, although it changes inside a unit cell. Taking the relation $H = -i/k_0(\partial E/\partial z)$ between magnetic and electric fields in the wave into account, we find

$$\zeta^{\pm} = \pm\frac{k_B}{k_0} - \frac{i}{k_0}\frac{\partial \ln f^{\pm}}{\partial z}\,.$$

The second term is a periodic function of z and corresponds to the contribution from the preexponential of the Bloch wave.

In the absence of losses and gains, the impedance $Z^{\pm}$ has complex values in the allowed band and purely imaginary values in the forbidden band [29]. The wave number k_B respectively takes real and complex values. This determines the main difference between the allowed and forbidden bands. The appearance of an imaginary part of the dielectric constant blurs band boundaries, but basic regularities are qualitatively preserved.

The rereflection process (the Airy series) is constructed as follows. The wave incident from the vacuum and the reflected wave with respective impedances $+1$ and -1 generate a Bloch wave inside a PC with the impedance $Z^{+} = 1/\zeta^{+}$ and the electric field amplitude $t_L = 2/(\zeta^{+} + 1)$ (see Fig. 3). This wave propagates in the PC, acquiring the factor $\exp(i\delta)$, $\delta = k_B N(d_1 + d_2)$, at the PC end. Then the wave is reflected from the right boundary; the reflected wave has the impedance $Z^{-} = 1/\zeta^{-}$ and the transmitted wave has the impedance $Z = 1$. The coefficient of transmission of the E^{+} wave into the vacuum is $t_R = (\zeta^{-} - \zeta^{+})/(\zeta^{-} - 1)$, and hence the amplitude of the first transmitted partial wave is $\tau_1 = t_L t_R \exp(i\delta)$. In this case, the reflection coefficient of the right boundary is $r_R = (1 - \zeta^{+})/(\zeta^{-} - 1)$. Then the E^{-} wave propagates through the PC layer and is reflected from the left boundary with the coefficient $r_L = -(1 + \zeta^{-})/(1 + \zeta^{+})$. The reflected E^{+} wave again propagates through the PC layer, and therefore the second partial wave escaping from the PC has the amplitude $\tau_2 = q\tau_1$, where

$$q = r_R r_L \exp(2i\delta)\,. \tag{12}$$

Further iterations are performed similarly, and the nth partial wave has the amplitude $\tau_n = q^{n-1}\tau_1$. As a result, the transmission coefficient can be represented as the series

$$t = t_L t_R \exp(i\delta)\sum_{n=0}^{\infty} q^n\,. \tag{12a}$$

The formal summation of this series gives the expression

$$t = \frac{t_L t_R \exp\left[ik_B N(d_1 + d_2)\right]}{1 - r_L r_R \exp\left[2ik_B N(d_1 + d_2)\right]}\,, \tag{12b}$$

which, as can be easily verified, identically coincides with the result obtained by the T-matrix method (if the E^{+} wave is treated as a wave propagating from the vacuum to the PC, i.e., as the 'incident' wave in the notation introduced in Section 3.2).

Further, a complete analogy with the case of a single gain layer is observed: the divergence of the Airy series in incident waves at some frequency is not a sufficient condition for lasing. Moreover, as we show below, this condition is necessary only when the pumping frequency ω_0 lies in the allowed band of the PC. When the pumping frequency lies in the forbidden band, the necessary condition for lasing onset is related to the divergence of the Airy series in counter waves.

4.2 Lasing in the allowed band of photonic crystals

The signs of the real and imaginary parts of k_B are opposite. The incident wave is amplified during its propagation in a PC. The convergence boundary of the Airy series, on which all the poles of the transfer function are located, is determined, as for a single gain layer, by the condition $|q| = 1$ [with q in (12)].

We note the principal difference between the case of a layer consisting of one PC cell and the case of a homogeneous layer. If pumping is absent and we neglect losses, we have the dependence shown in Fig. 10a instead of the dependence in Fig. 6a. Regions where the Airy series in incident waves diverges are shown in grey. For one cell, three such regions exist. One of them surrounds the region of real frequencies corresponding to the forbidden PC band. A region in the upper half-plane also appears. An increase in the number of layers leads to the joining of these regions and filling of the region with the real part of the frequency belonging to the forbidden band (Fig. 10c). However, as in the case of a single layer, all the poles lie in the lower half-plane.

Because the value of q in (12) increases as the number N of layers increases, the divergence condition for the Airy series can be treated as the excess of the number of layers over a critical value, $N > N_{cr}$, similarly to the critical thickness of a homogeneous layer. Indeed, for $N < N_{cr}$, the Airy method for incident waves and the Fresnel method (the T-matrix method) give the same result; for $N > N_{cr}$, the calculation by the T-matrix method gives a finite result, but the Airy series in incident waves diverges. The function $N_{cr}(\omega)$, being a real function of the complex variable ω, defines the curve $|q(N_{cr}(\omega))| = 1$ in the complex frequency plane.

Pumping changes not only the imaginary but also the real part of the dielectric constant. This leads to a deformation of the curve $|q(\omega)| = 1$, but the dynamics of the poles as a function of the thickness (the number of cells) resembles that in the case of a single gain layer (Fig. 11).

Singularities occur only near the forbidden band boundary. As could be expected, the critical number $N_{cr}(\omega)$ of layers decreases in allowed bands near their boundaries because of the decrease in the group velocity of Bloch waves. We note that this effect is more strongly manifested at the bottom boundary of the forbidden band due to the concentration of the electric field energy in gain layers with large ε values (the Borrmann effect [74]), and hence lasing can be more readily obtained near the bottom boundary of the forbidden band (Fig. 12).

4.3 Lasing in the forbidden band of a photonic crystal

If the pump frequency lies in the forbidden band, then, unlike in the case of the allowed band, the dependence of the lasing threshold on the number of PC cells is nonmonotonic (Fig. 13). This is explained by the fact that the forbidden

[4] Below, we assume that preexponential functions are normalized such that they are equal to unity at $z = 0$. The relation between $\zeta^{\pm}$ and k_B is discussed in detail in [29].

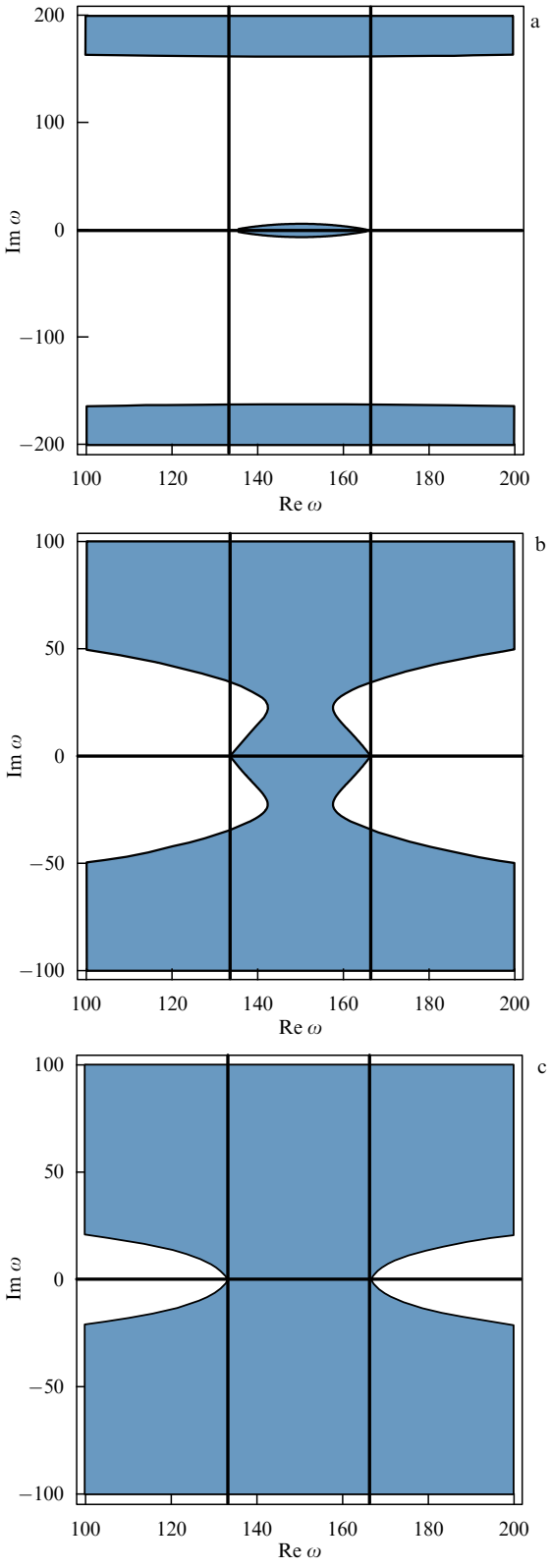

Figure 10. (See in color online.) Formation of the forbidden band in a PC; (a) one cell, (b) two cells, (c) four cells. Gains and losses are absent.

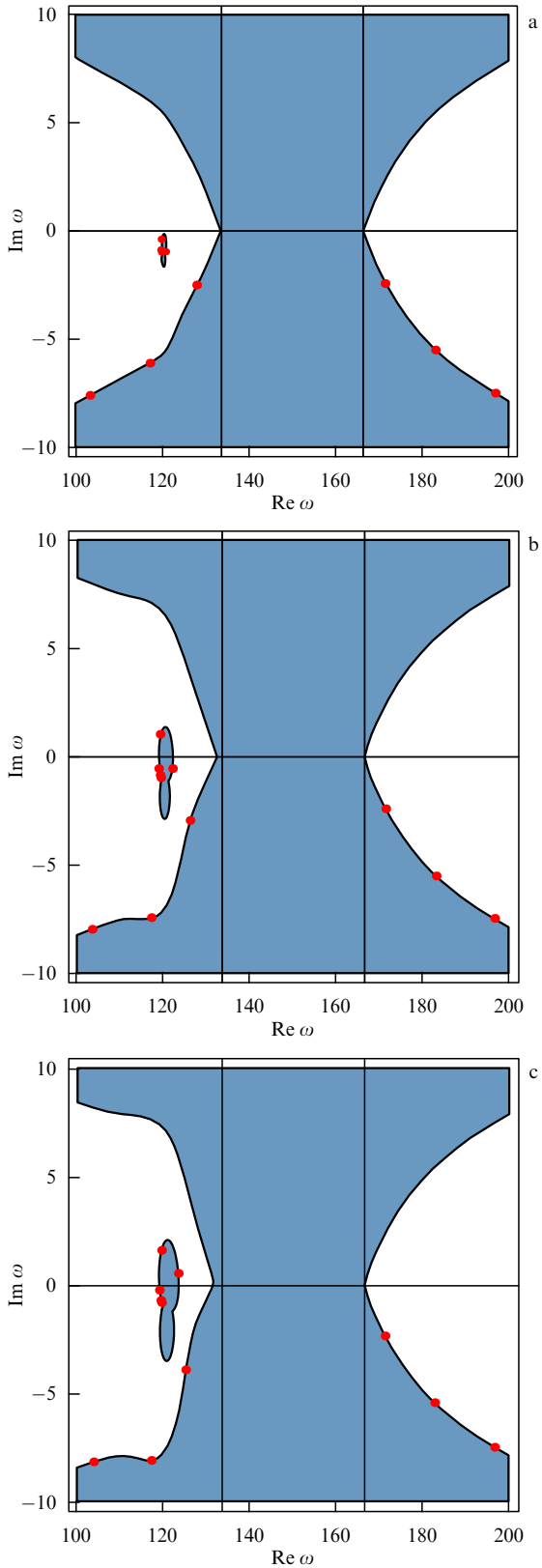

Figure 11. (See in color online.) Position of the curve $|q| = 1$ in the complex frequency plane (solid curve) and positions of poles (indicated by circles) for dielectric constants of the gain medium (a) $2 - 0.05i$, (b) $2 - 0.12i$, and (c) $2 - 0.18i$.

band exists only in an infinite PC. The properties of the forbidden band are formed when increasing the number of PC cells. For small thicknesses, the dependence on the thickness resembles that in the case of the allowed band (see Section 4.2). Below, we treat allowed and forbidden bands not only as sets of real frequencies but also as the bands corresponding to them in the complex frequency plane.

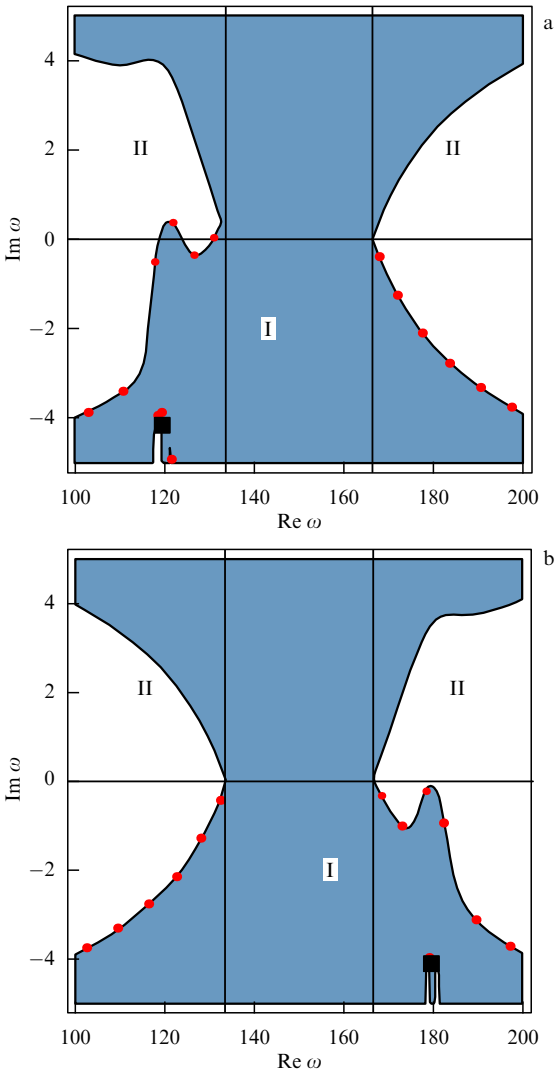

Figure 12. (See in color online.) Arrangements of poles of the response function of a PC in the complex frequency plane for pump frequencies in (a) the lower and (b) the upper boundaries of the forbidden band. Grey and white regions respectively indicate convergence regions of the Airy series in incident and counter waves.

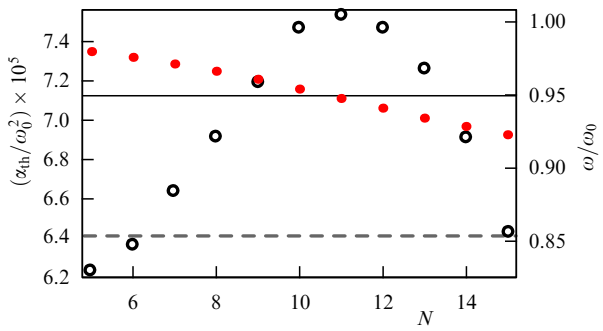

Figure 13. The threshold value α_{th} (circles) and the lasing frequency ω normalized to the central frequency ω_0 of the forbidden band (filled circles) as functions of the number N of layers. The dashed straight line indicates the forbidden band boundary.

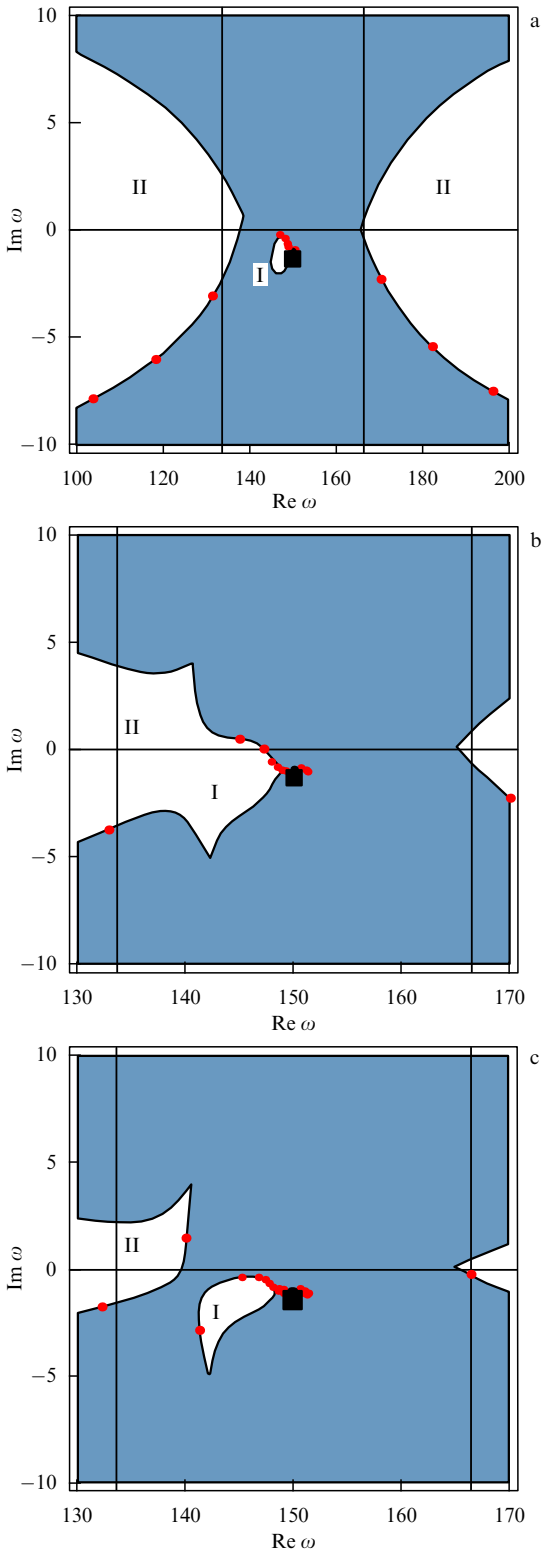

Figure 14. (See in color online.) Arrangement of poles of the PC response function in the complex frequency plane (indicated by circles) for different numbers of layers. The square indicates a pole of the dielectric constant. The Airy series in incident waves converges in white regions and diverges in grey regions: (a) 10 PC cells, (b) 12 PC cells, (c) 14 PC cells.

For sufficiently large PC thicknesses, when the dependence of the threshold on the thickness changes, the topology of the convergence region of the Airy series also changes. Now the convergence boundary for the Airy series at forbidden band frequencies surrounds the convergence region of the series in incident waves (white region I in Fig. 14a). Simultaneously, the convergence region of the same series exists in the allowed band (region II). Outside

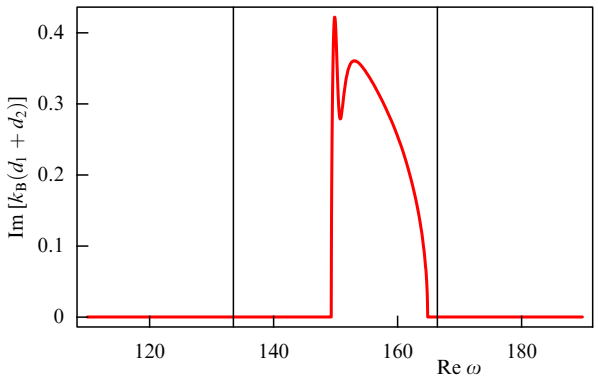

Figure 15. (See in color online.) Dependence of the imaginary part of k_B of an auxiliary PC on the carrier frequency of the incident train. Vertical straight lines indicate the boundaries of the forbidden band for the PC without gain.

these regions, the Airy series in incident Bloch waves (12b) diverges. However, lasing does not appear in the case of weak pumping, because all poles of the transfer function lie below the real frequency axis, in the vicinity of the dielectric constant pole $\varepsilon_{\text{gain}}$ (Fig. 14a).

As the pump level is increased, region I increases (Fig. 14b) such that its boundary sooner or later intersects the real axis, and one of the poles comes out to the upper half-plane. Lasing appears at some frequency in the forbidden band (Fig. 14b). In this case, the convergence region mentioned above can either remain isolated or merge with a similar region existing in the allowed band (Fig. 14b). In the second case, poles can pass from the forbidden band to the allowed band. However, as the number of layers is increased, the regions again separate (Fig. 14c). As the number of layers is increased further, poles located at the boundary of region I move downward, while poles located at the boundary of region II move upward. When the number of layers is large, lasing can occur only at the boundary of region II.

The passage of the pole from region I to region II leads to a nonmonotonic dependence of the threshold pump on the number of layers (see Fig. 13). As long as the pole is located at the boundary of region I, the increase in the number of layers leads to an increase in α_{th} (open circles in Fig. 13). But after the pole passes to region II (dark circles in Fig. 13), the behavior is reversed. In this case, the lasing frequency monotonically shifts to the lower boundary of the forbidden band.

Hence, when the gain line is located in region I, lasing is possible only when the number of layers is small: $N < N_{\text{cr}}$. However, the increase in the number of layers eventually leads only to lasing at frequencies in region II. This is possible because of the finite width of the gain line.

Notably, if the gain line width is sufficiently small, regions I and II do not merge (Fig. 14a). In this case, poles cannot pass from region I to region II, and the increase in the number of layers suppresses lasing. Nevertheless, lasing eventually appears in the allowed region upon increasing the number of layers due to the finite width of the gain line.

We note that region II covers both the allowed and forbidden bands. This is explained by the fact that the increase in the gain parameter α changes the dielectric constant $\varepsilon_{\text{gain}}$ [see (2d)]. The appearance of lasing in the part of region II that lies in the forbidden band can therefore be interpreted as a change in the band structure of a PC. Indeed, when we change the gain parameter α, both the imaginary and real parts of $\varepsilon_{\text{gain}}(\alpha)$ change. If we consider an auxiliary PC in which the gain layer is replaced by a layer with the dielectric constant $\operatorname{Re}\varepsilon_{\text{gain}}(\alpha)$, the forbidden band of this auxiliary PC would be narrower than that of the original PC with $\alpha = 0$ (Fig. 15). In this case, region II entirely lies in the allowed band of the auxiliary PC.

Hence, for $N < N_{\text{th}}(\alpha)$, the upper half-plane always has at least one pole, and lasing is therefore observed. For $N_{\text{th}} < N < N_{\text{las}}(\alpha)$, the poles of the transfer function can enter the upper half-plane and come out of it; in this case, lasing alternately starts and terminates. For $N_{\text{las}} < N < N_{\text{cr}}(\alpha)$, the Airy series in incident waves does not converge [curve (12) touches the real frequency axis from below], but poles are absent in the upper half-plane, and lasing is not observed. For $N > N_{\text{cr}}(\alpha)$, the Airy series in incident waves converges [curve (12) does not touch the real frequency axis from below].

5. Oblique incidence of light on a gain layer

We next consider the case of an oblique incidence of a wave on a gain layer surrounded by a medium with a dielectric constant ε_{e}. Fresnel formulas (3) and Airy series (4), (5), which we obtained for normally incident light, have the same form after the replacement

$$\sqrt{\varepsilon_{\text{gain}}} \to \sqrt{\varepsilon_{\text{gain}} - \varepsilon_{\text{e}} \sin^2\phi}$$

and

$$Z_2 \to \sqrt{\varepsilon_{\text{gain}} - \varepsilon_{\text{e}} \sin^2\phi}\,, \qquad Z_1 \to \sqrt{\varepsilon_{\text{e}}}\,\cos\phi$$

for the s-polarization, and

$$Z_2 \to \frac{\sqrt{\varepsilon_{\text{gain}} - \varepsilon_{\text{e}} \sin^2\phi}}{\varepsilon_{\text{gain}}}\,, \qquad Z_1 \to \frac{\cos\phi}{\sqrt{\varepsilon_{\text{e}}}}$$

for the p-polarization, where ϕ is the angle of incidence.

It follows from the Fresnel formulas that the transmission coefficient T of a gain or dissipative layer tends to zero upon increasing the layer thickness d, while the reflection coefficient R tends to a nonzero constant. In a semi-infinite gain or dissipative medium, only one wave decreasing with the distance from the boundary remains. The difference between the dissipative and gain media consists in the direction of the Poynting vector: in the first case, this vector is directed from the boundary to the interior of the half-space, while in the second case, it is directed to the boundary.

As in the case of normal incidence, Fresnel formulas become invalid when lasing appears, i.e., in the presence of poles of the response function in the upper complex frequency half-plane. The position of poles is determined by the equation

$$q = \left(\frac{\sqrt{\varepsilon_{\text{gain}} - \varepsilon_{\text{e}} \sin^2\phi} - \sqrt{\varepsilon_{\text{e}}}\,\cos\phi}{\sqrt{\varepsilon_{\text{gain}} - \varepsilon_{\text{e}} \sin^2\phi} + \sqrt{\varepsilon_{\text{e}}}\,\cos\phi}\right)^2 \times \exp\left(\frac{2\mathrm{i}\omega d}{c}\sqrt{\varepsilon_{\text{gain}} - \varepsilon_{\text{e}} \sin^2\phi}\right) = 1\,. \qquad (13)$$

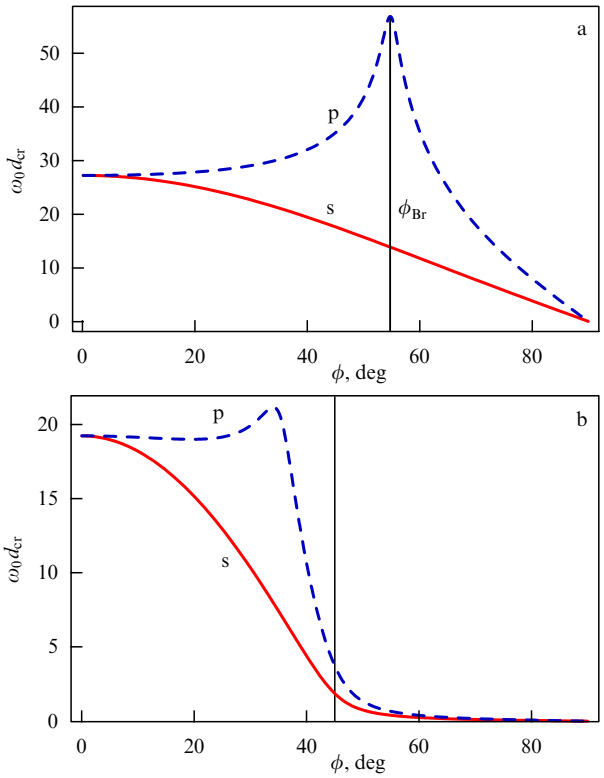

Figure 16. Angular dependences of the critical layer thickness for the s-polarization (solid curves) and p-polarization (dashed curves). (a) The nonresonance part of the dielectric constant $\varepsilon_0 = 2$ of a layer [see Eqn (2d)] in the vacuum. (b) A layer with $\varepsilon_0 = 1$ in a dielectric with $\varepsilon_e = 2$.

The poles of the response function are located on the curve determined from the amplitude conditions of lasing:

$$|r_\infty|^2 \exp\left(\frac{2\omega d}{c}\,\mathrm{Im}\sqrt{\varepsilon_{gain} - \varepsilon_e \sin^2\phi}\right) = 1\,, \qquad (14)$$

$$r_\infty = \frac{Z_1 - Z_2}{Z_1 + Z_2}\,.$$

To determine the gain layer thickness $d_{las}(\phi)$ at which lasing begins, it is convenient to follow the evolution of curve (14) in the complex frequency plane as the layer thickness changes. Unlike normal incidence, oblique incidence can correspond to two fundamentally different cases.

If the gain medium is surrounded by a medium with a lower optical density, $\mathrm{Re}\,\varepsilon_{gain} > \varepsilon_e$, the situation is identical to the case of normal incidence. For $d < d_{cr}(\phi)$, the Airy series in incident waves converges, while for $d > d_{cr}(\phi)$, it diverges, and the poles of the transfer function can pass to the upper half-plane. The critical thickness of the layer at which lasing appears depends on the angle of incidence. For the p-polarization, $d_{las}(\phi) \to \infty$ for the incidence of light at the Brewster angle ϕ_{Br} (Fig. 16a). This is explained by the fact that when the Brewster condition is exactly satisfied, reflection is absent and the layer is no longer a resonator. Because of the gain, the dielectric constant of the layer has an imaginary part, and therefore its impedance differs from unity. Hence, $d_{las}(\phi_{Br})$ preserves a finite value.

But if the layer is located in a dielectric with a higher optical density, $\mathrm{Re}\,\varepsilon_{gain} < \varepsilon_e$, a region of total internal reflection appears (to the right of the vertical line in Fig. 16b). In this region, d_{cr} decreases with increasing the angle of incidence, but this does not mean that the region $\phi > \phi_{TIR}$ (ϕ_{TIR} is the angle of total internal reflection) facilitates lasing, because this is only the amplitude condition, and the phase condition (the passage of a pole) is also required.

For angles of incidence ϕ smaller than ϕ_{TIR}, curve (14) and the poles of the response function behave similarly to those in the case of normal incidence (Fig. 17).

For angles of incidence above the critical angle, the convergence and divergence regions of the Airy series change places (Fig. 17e). As the layer thickness increases, the region where the Airy series in increasing waves converges decreases, and therefore curve (14), lying between convergence regions, descends in the complex frequency plane with increasing the layer thickness. Hence, for angles of incidence greater than the total internal reflection angle, lasing can be observed only in the gain layer with a small thickness, and it disappears upon increasing the layer thickness, similarly to the case of the forbidden band in a PC. Poles located on curve (14) move clockwise along this curve with increasing the angle of incidence (see Fig. 17) [100], and occur near the transition frequency ω_0 for $\phi \to \phi_{TIR}$.

It is interesting to note that the angle at which convergence regions change places is exactly equal to the total internal reflection angle in the absence of gain: $\phi_{cr} = \phi_{TIR} = \arcsin\sqrt{\varepsilon_0/\varepsilon_e}$. Here, ε_0 is the real part of the dielectric constant with dispersion neglected [see (2d)]. This value of the critical angle was obtained in [41, 100] and seems strange at first glance. The value $\phi_{cr} = \arcsin\sqrt{\mathrm{Re}\,\varepsilon_{gain}(\omega)/\varepsilon_e}$ would be more expected. We note, however, that the inversion of convergence regions for the Airy series [see Fig. 17] is determined by the properties of the system for $\omega \to \infty$, where $\varepsilon_{gain} \to \varepsilon_0$ due to the finite width of the gain line. In this case, the incident wave is not amplified, and for angles exceeding the total internal reflection angle $(\varepsilon_0 - \varepsilon_e \sin^2\phi) < 0$, the series in decreasing waves converges at real frequencies [41, 100].

Therefore, for $\phi < \phi_{cr}$, lasing appears as the gain layer thickness increases, while for $\phi > \phi_{cr}$, lasing is possible only in a thin gain layer. The angle $\phi_{cr} = \phi_{TIR} = \arcsin\sqrt{\varepsilon_0/\varepsilon_e}$ at which one type of behavior passes into another is determined by the value of the dielectric constant with dispersion neglected [41].

6. Conclusions

We have emphasized in this review that as long as lasing is absent in a layered system containing gain layers, the use of the effective dielectric constant ε_{gain} with a negative imaginary part is valid for the description of the system.

The hierarchy of gain layer thicknesses has the form $d_0 < d_{cr} < d_{las} < d_{th}$. In all the cases considered here, a gain layer thickness d_0 or a number N_0 of unit cells in a PC exist beginning from which the reflection coefficient of the layer exceeds unity. Then, as the system thickness is increased, the critical thickness d_{cr} of the gain layer is reached above which the Airy series in incident waves diverges. For layer thicknesses smaller than d_{cr}, the Airy series converges to the result obtained by the Fresnel method (the solution of a linear wave equation), which in turn coincides with the numerical solution of the Maxwell–Bloch equations.

A different situation occurs when the threshold value d_{las} is exceeded and lasing begins. Instead of the linear state predicted by the Fresnel approach, a nonlinear stationary

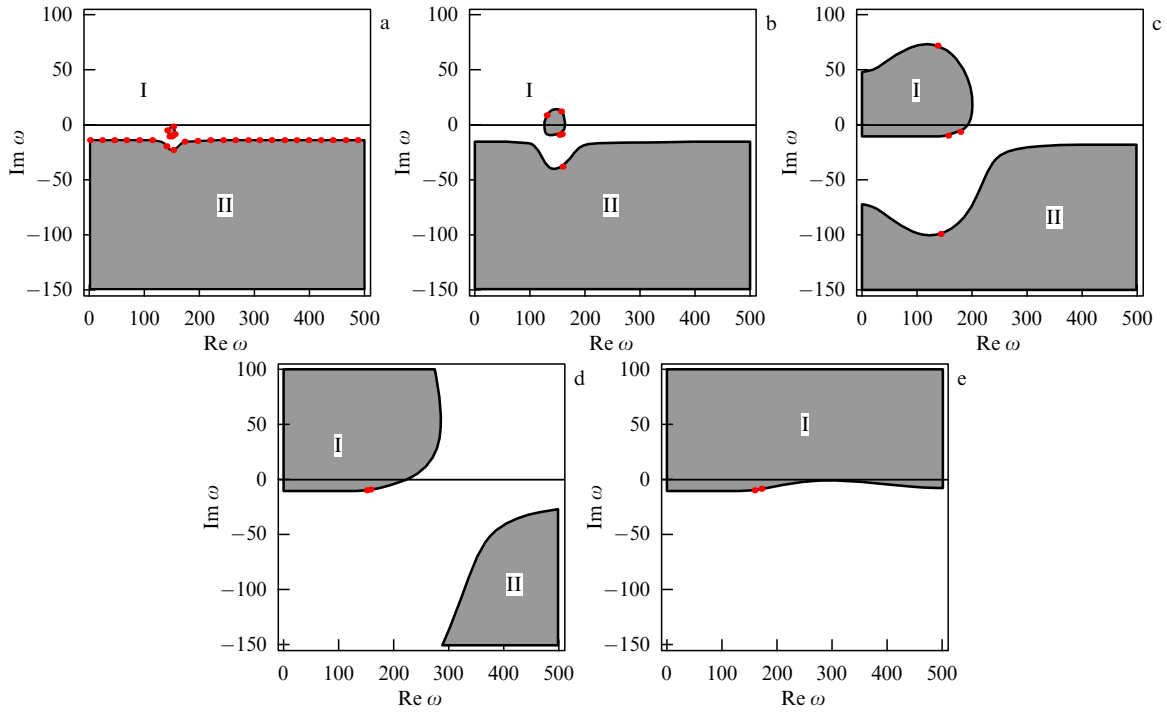

Figure 17. (See in color online.) Position of the poles of the transfer function in the complex plane for different angles of incidence. The divergence regions of the Airy series in incident waves for the normal incidence are shown in grey: (a) normal incidence, $\phi = 0$, (b) angle of incidence $\phi = 0.9\,\phi_{\mathrm{TIR}}$, (c) $\phi = 0.99\,\phi_{\mathrm{TIR}}$, (d) $\phi = 0.999\,\phi_{\mathrm{TIR}}$, (e) angle of incidence is greater than the angle of total internal reflection, $\phi = 1.01\,\phi_{\mathrm{TIR}}$.

solution appears (Fig. 4c). In this case, even if the field intensity in the Fresnel solution is small, and it would seem that a field-induced change in the inverse population can be neglected, Maxwell–Bloch equations (1) yield a solution with a large amplitude at which nonlinearity becomes decisive. The exact condition for the appearance of lasing is the passage of the poles of the linear response function $g(\omega)$ in (3) to the upper half-plane of complex frequencies ω.

The construction of the Airy series quite well describes the propagation of a semi-infinite wave train through a layer of matter. But it should be performed differently for a gain medium in the cases $d < d_{\mathrm{cr}}$ and $d > d_{\mathrm{cr}}$. Indeed, the Airy series is constructed by using the reflection coefficient r_∞ in the problem of the reflection of a plane wave from the half-space. The value of r_∞ depends on the wave with which a wave incident from the vacuum is matched in the layer. If, as is usually accepted for dissipative media [88], we take a wave transferring energy inside a layer, i.e., the incident wave, then for $d < d_{\mathrm{cr}}$, the modulus of the denominator of the geometric progression $q = r_\infty^2 \exp(2\mathrm{i}\delta)$ is smaller than unity, and the Airy series in incident waves converges to expression (3b) obtained in the Fresnel approach.

But if the Airy series is constructed assuming that the solution in a semi-infinite medium is a counter wave [42], then the impedance Z_2 and the complex phase δ in (4a) and (4b) change sign. As a result, the denominator of the progression becomes equal to $1/q$, and for $d > d_{\mathrm{cr}}$, already the Airy series in counter waves (6b) converges, as follows from calculations by the Fresnel method.

The analysis performed here shows that result (3b) obtained by the Fresnel method can be treated as an analytic continuation of the sum of Airy series (5) to the region $d > d_{\mathrm{cr}}(\omega)$ in the complex frequency plane (shaded regions in Fig. 6). In other words, for $d < d_{\mathrm{cr}}$, it is necessary to use the Airy series in incident waves, while for $d > d_{\mathrm{cr}}$, it must be used in counter waves. We note that for $d = d_{\mathrm{cr}}$ ($|q| = 1$), neither of the series converges, but if $q \neq 1$, then the upper and lower limits for $d \to d_{\mathrm{cr}} \pm 0$ coincide.

Passing from the Airy series in incident waves to the Airy series in counter waves is equivalent to the analytic continuation of the function $1/(1-q)$ from the vicinity of $q = 0$, where

$$\frac{1}{1-q} = \sum_n q^n\,,$$

to the vicinity of $|q| = \infty$, where [56]

$$\frac{1}{1-q} = -\frac{1/q}{1-1/q} = -\frac{1}{q}\sum_{n=0}^{\infty}\left(\frac{1}{q}\right)^n.$$

Thus, we obtain the complete correspondence between the Airy series and the result of the Fresnel approach, which is the same analytic function whose expansion in a power series represents the Airy series. Similarly to the modified Fresnel approach, a sum of residues in poles determined by the condition $q(\omega) = 1$ must be added to the Airy series in counterwaves. This adds terms infinitely increasing with time in the parameter regions where lasing occurs.

A physical parameter determining the lasing onset condition is the path along which a beam propagates in a layer. In the case of oblique incidence, this path differs from the layer thickness. As a result, the smaller values of thicknesses d_0, d_{cr}, d_{las}, and d_{th} correspond to modes propagating at angles. In particular, these values tend to zero when the angle of incidence tends to $\pi/2$ (see Fig. 17). The expansion of a beam with a finite aperture in plane waves always contains waves with angles of incidence close to $\pi/2$. It is necessary to take into account that the path of such waves is restricted by the width of the beam or by the transverse size of

the system. Indeed, pumping is performed not in the entire plane but in the restricted region of the layer, as in the case of VCSELs [1–6]. Escaping from this region, the waves fall into the absorption region.

In the case of an oblique incidence of an electromagnetic wave, the effect of the Brewster phenomenon and total internal reflection is significant. For a nonzero imaginary part of $\varepsilon_{\text{gain}}$, the Brewster angle and the angle of total internal reflection are complex. But it turns out that in the case of total internal reflection, a real critical angle ϕ_{cr} exists, equal to the angle of total internal reflection ϕ_{TIR} in the absence of pumping, and the behavior of the system above and below this angle is qualitatively different. For angles of incidence smaller than this angle, the dependences of all the quantities on the layer thickness are similar to those in the case of normal incidence on the layer or on a PC in the allowed band, namely, the characteristic thicknesses d_0, d_{cr}, d_{las}, and d_{th} exist. In the case of incidence at angles greater than the critical angle, all the dependences on the layer thickness are similar to those in PCs at frequencies in the forbidden band: d_0 always exists, d_{cr} and d_{las} do not exist for all pump levels, and d_{th} is absent. An increase in the layer thickness eventually leads to the interruption of lasing.

Acknowledgments

The authors thank A N Lagarkov, V N Kisel', and Yu E Lozovik for the useful discussions. This work was partially supported by the Russian Foundation for Basic Research (grants No. 10-02-91750-AF, 11-02-92475-ISTI, 12-02-01093), and by a PSC-CUNY grant.

References

1. Iga K *IEEE J. Selected Topics Quantum Electron.* **6** 1201 (2000)
2. Botez D, Scifres D R (Eds) *Diode Laser Arrays* (Cambridge: Cambridge Univ. Press, 2005)
3. Kawai S (Ed.) *Handbook of Optical Interconnects* (Boca Raton: CRC Press/Taylor & Francis Group, 2005)
4. Yu S F *Analysis and Design of Vertical Cavity Surface Emitting Lasers* (Hoboken, NJ: Wiley-Interscience, 2003)
5. Wilmsen C W, Temkin H, Coldren L A (Eds) *Vertical-Cavity Surface-Emitting Lasers: Design, Fabrication, Characterization, and Applications* (Cambridge: Cambridge Univ. Press, 1999)
6. Cheng J, Dutta N K (Eds) *Vertical-Cavity Surface-Emitting Lasers: Technology and Applications* (Amsterdam: Gordon & Breach, 2000)
7. Asatryan A A et al. *Phys. Rev. B* **57** 13535 (1998)
8. Bulgakov S A, Nieto-Vesperinas M *Waves Random Media* **10** 373 (2000)
9. Frank R, Lubatsch A, Kroha J *Phys. Rev. B* **73** 245107 (2006)
10. Heinrichs J *Phys. Rev. B* **56** 8674 (1997)
11. Jiang X, Li Q, Soukoulis C M *Phys. Rev. B* **59** R9007 (1999)
12. Joshi S K, Jayannavar A M *Phys. Rev. B* **56** 12038 (1997)
13. Nam C-K, Zhang Z-Q *Phys. Rev. B* **66** 073101 (2002)
14. Paasschens J C J, Misirpashaev T Sh, Beenakker C W J *Phys. Rev. B* **54** 11887 (1996)
15. Ramakrishna S A et al. *Phys. Rev. B* **62** 256 (2000)
16. Yamilov A et al. *Phys. Rev. B* **71** 092201 (2005)
17. Datta P K *Phys. Rev. B* **59** 10980 (1999)
18. Dowling J P et al. *J. Appl. Phys.* **75** 1896 (1994)
19. Jiang X, Soukoulis C M *Phys. Rev. Lett.* **85** 70 (2000)
20. Feng Y, Ueda K *Opt. Express* **12** 3307 (2004)
21. Pendry J B *Phys. Rev. Lett.* **85** 3966 (2000)
22. Veselago V G *Usp. Fiz. Nauk* **92** 517 (1967) [*Sov. Phys. Usp.* **10** 509 (1968)]
23. Ramakrishna S A, Pendry J B *Phys. Rev. B* **67** 201101(R) (2003)
24. Fang A, Koschny T, Soukoulis C M *J. Opt.* **12** 024013 (2010)
25. Xiao S et al. *Nature* **466** 735 (2010)
26. Cai W, Shalaev V *Optical Metamaterials. Fundamentals and Applications* (New York: Springer, 2010)
27. Wuestner S et al. *Phys. Rev. Lett.* **105** 127401 (2010)
28. Vinogradov A P, Dorofeenko A V, Zouhdi S *Usp. Fiz. Nauk* **178** 511 (2008) [*Phys. Usp.* **51** 485 (2008)]
29. Vinogradov A P, Dorofeenko A V, Merzlikin A M, Lisyansky A A *Usp. Fiz. Nauk* **180** 249 (2010) [*Phys. Usp.* **53** 243 (2010)]
30. Shatrov A D *Radiotekh. Elektron.* **52** 1430 (2007) [*J. Commun. Technol. Electron.* **52** 1324 (2007)]
31. Mozjerin I et al. *Opt. Lett.* **35** 3240 (2010)
32. Sarychev A K, Pukhov A A, Tartakovsky G *PIERS Online* **3** 1264 (2007)
33. Sarychev A K, Tartakovsky G *Phys. Rev. B* **75** 085436 (2007)
34. Gabitov I R, Kennedy B, Maimistov A I *IEEE J. Selected Topics Quantum Electron.* **16** 401 (2010)
35. Lagarkov A N et al. *Usp. Fiz. Nauk* **179** 1018 (2009) [*Phys. Usp.* **52** 959 (2009)]
36. Noginov M A et al. *Opt. Express* **16** 1385 (2008)
37. Khanin Ya I *Osnovy Dinamiki Lazerov* (Fundamentals of Laser Dynamics) (Moscow: Fizmatlit, 1999)
38. Hu X et al. *Phys. Rev. B* **77** 205104 (2008)
39. Solimeno S, Crosignani B, DiPorto P *Guiding, Diffraction, and Confinement of Optical Radiation* (Orlando: Academic Press, 1986) [Translated into Russian (Moscow: Mir, 1989)]
40. Kolokolov A A *Usp. Fiz. Nauk* **169** 1025 (1999) [*Phys. Usp.* **42** 931 (1999)]
41. Vainshtein L A *Usp. Fiz. Nauk* **118** 339 (1976) [*Sov. Phys. Usp.* **19** 189 (1976)]
42. Kolokolov A A *Pis'ma Zh. Eksp. Teor. Fiz.* **21** 660 (1975) [*JETP Lett.* **21** 312 (1975)]
43. Romanov G N, Shakhidzhanov S S *Pis'ma Zh. Eksp. Teor. Fiz.* **16** 298 (1972) [*JETP Lett.* **16** 210 (1972)]
44. Boiko B B, Petrov N S *Otrazhenie Sveta ot Usilivayushchikh i Nelineinykh Sred* (Reflection of Light from Amplifying and Nonlinear Media) (Minsk: Nauka i Tekhnika, 1988)
45. Dolling G et al. *Opt. Lett.* **31** 1800 (2006)
46. Wegener M et al. *Opt. Express* **16** 19785 (2008)
47. Meinzer N et al. *Opt. Express* **18** 24140 (2010)
48. Dong Z-G et al. *Appl. Phys. Lett.* **96** 044104 (2010)
49. Fang A et al. *Phys. Rev. B* **79** 241104(R) (2009)
50. Fang A, Koschny Th, Soukoulis C M *Phys. Rev. B* **82** 121102(R) (2010)
51. Chen X et al. *Phys. Rev. E* **70** 016608 (2004)
52. Smith D R et al. *Phys. Rev. E* **71** 036617 (2005)
53. Menzel C et al. *Phys. Rev. B* **77** 195328 (2008)
54. Franceschetti G *Alta Frequenza* **36** 757 (1967)
55. Smith D R, Schurig D *Phys. Rev. Lett.* **90** 077405 (2003)
56. Lavrent'ev M A, Shabat B V *Metody Teorii Funktsii Kompleksnogo Peremennogo* (Methods of the Theory of Functions of a Complex Variable) (Moscow: Nauka, 1965)
57. Lagarkov A N, Kissel V N *Phys. Rev. Lett.* **92** 077401 (2004)
58. Landau L D, Lifshitz E M *Elektrodinamika Sploshnykh Sred* (Electrodynamics of Continuous Media) (Moscow: Fizmatlit, 2003) [Translated into English (Oxford: Pergamon Press, 1984)]
59. Lebedev S A, Volkov V M, Kogan B Ya *Opt. Spektrosk.* **35** 976 (1973)
60. Kogan B Ya, Volkov V M, Lebedev S A *Pis'ma Zh. Eksp. Teor. Fiz.* **16** 144 (1972) [*JETP Lett.* **16** 100 (1972)]
61. Goos F, Hänchen H *Ann. Physik* **436** 333 (1947)
62. Goos F, Lindberg-Hänchen H *Ann. Physik* **440** 251 (1949)
63. Bergman D J, Stockman M I *Phys. Rev. Lett.* **90** 027402 (2003)
64. Andrianov E S et al. *Opt. Express* **19** 24849 (2011)
65. Andrianov E S et al. *Opt. Lett.* **36** 4302 (2011)
66. Andrianov E S et al. *Phys. Rev. B* **85** 165419 (2012)
67. Andrianov E S et al. *Phys. Rev. B* **85** 035405 (2012)
68. Lisyansky A A et al. *Phys. Rev. B* **84** 153409 (2011)
69. Stockman M I *Phil. Trans. R. Soc. A* **369** 3510 (2011)
70. Andrianov E S, Pukhov A A, Dorofeenko A V, Vinogradov A P *Radiotekh. Elektron.* **57** 114 (2012) [*J. Commun. Technol. Electron.* **57** 106 (2012)]
71. Plum E et al. *Opt. Express* **17** 8548 (2009)
72. Kolokolov A A, Skrotskii G V *Usp. Fiz. Nauk* **162** (12) 165 (1992) [*Sov. Phys. Usp.* **35** 1089 (1992)]
73. Vinogradov A P, Dorofeenko A V *Radiotekh. Elektron.* **50** 1246 (2005) [*J. Commun. Technol. Electron.* **50** 1153 (2005)]

74. Vinogradov A P et al. *Phys. Rev. B* **80** 235106 (2009)
75. Vinogradov A P, Dorofeenko A V *Opt. Commun.* **256** 333 (2005)
76. Mandel L, Wolf E *Optical Coherence and Quantum Optics* (Cambridge: Cambridge Univ. Press, 1995) [Translated into Russian (Moscow: Fizmatlit, 2000)]
77. Heitler W *The Quantum Theory of Radiation* (Oxford: Clarendon Press, 1954) [Translated into Russian (Moscow: IL, 1956)]
78. Oraevsky A N *Kvantovaya Elektron.* **29** (11) 137 (1999) [*Quantum Electron.* **29** 975 (1999)]
79. Pantell R H, Puthoff H E *Fundamentals of Quantum Electronics* (New York: Wiley, 1969) [Translated into Russian (Moscow: Mir, 1972)]
80. Scully M O, Zubairy M S *Quantum Optics* (Cambridge: Cambridge Univ. Press, 1997) [Translated into Russian (Moscow: Fizmatlit, 2003)]
81. Lukš A, Peřinová V *Quantum Aspects of Light Propagation* (Dordrecht: Springer, 2009)
82. Erneux T, Glorieux P *Laser Dynamics* (New York: Cambridge Univ. Press, 2010)
83. Zyablovsky A A, Dorofeenko A V, Vinogradov A P, Pukhov A A *Photon. Nanostruct. Fundament. Appl.* **9** 398 (2011)
84. Kivshar Y S, Agrawal G P *Optical Solitons*: *from Fibers to Photonic Crystals* (Amsterdam: Academic Press, 2003)
85. Zyablovsky A A, Dorofeenko A V, Pukhov A A, Vinogradov A P *Radiotekh. Elektron.* **56** 1142 (2011) [*J. Commun. Technol. Electron.* **56** 1139 (2011)]
86. Yariv A *Quantum Electronics* (New York: Wiley, 1975) [Translated into Russian (Moscow: Sov. Radio, 1980)]
87. Jackson J D *Classical Electrodynamics* (New York: Wiley, 1962) [Translated into Russian (Moscow: Mir, 1965)]
88. Airy G B *Philos. Mag.* **2** 20 (1833)
89. Sturrock P A *Phys. Rev.* **112** 1488 (1958)
90. Skaar J *Phys. Rev. E* **73** 026605 (2006)
91. Vladimirov V S *Obobshchennye Funktsii v Matematicheskoi Fizike* (Generalized Functions in Mathematical Physics) (Moscow: Nauka, 1979)]
92. Vladimirov V S *Uravneniya Matematicheskoi Fiziki* (Equations of Mathematical Physics) (Moscow: Nauka, 1981) [Translated into English (Moscow: Mir, 1984)]
93. Sivukhin D V *Obshchii Kurs Fiziki* (General Course of Physics) Vol. 4 *Optika* (Optics) (Moscow: Fizmatlit, MFTI, 2002)
94. Butikov E I *Optika* (Optics) (Moscow: Vysshaya Shkola, 1986)
95. Born M, Wolf E *Principles of Optics* (Oxford: Pergamon Press, 1969) [Translated into Russian (Moscow: Nauka, 1970)]
96. Sommerfeld A *Vorlesungen über theoretische Physik* Bd. 4 *Optik* (Wiesbaden: Dieterich, 1950) [Translated into English: *Lectures on Theoretical Physics* Vol. 4 *Optics* (New York: Academic Press, 1954); Translated into Russian (Moscow: IL, 1953)]
97. Vaganov R B, Katsenelenbaum B Z *Osnovy Teorii Difraktsii* (Fundamentals of the Diffraction Theory) (Moscow: Nauka, 1982)
98. Weinstein L A *Otkrytye Rezonatory i Otkrytye Volnovody* (Open Resonators and Open Waveguides) (Moscow: Sov. Radio, 1966) [Translated into English (Boulder, Colo.: Golem Press, 1969)]
99. Bahlouli H et al. *Phys. Rev. B* **72** 094304 (2005)
100. Mantsyzov B I *Kogerentnaya i Nelineinaya Optika Fotonnykh Kristallov* (Coherfent and Nonlinear Optics of Photonic Crysyals) (Moscow: Fizmatlit, 2009)
101. Kurizki G et al., in *Progress in Optics* Vol. 42 (Ed. E Wolf) (Amsterdam: North-Holland, 2001) p. 93